

# WeEdit: A Dataset, Benchmark and Glyph-Guided Framework for Text-centric Image Editing

Hui Zhang<sup>1,2</sup> Juntao Liu<sup>1</sup> Zongkai Liu<sup>1,3</sup> Liqiang Niu<sup>1</sup> Fandong Meng<sup>1</sup>  
Zuxuan Wu<sup>2</sup> Yu-Gang Jiang<sup>2</sup>

<sup>1</sup>WeChat AI, Tencent, <sup>2</sup>Fudan University, <sup>3</sup>Sun Yat-sen University

## Abstract

Instruction-based image editing aims to modify specific content within existing images according to user-provided instructions while preserving non-target regions. Beyond traditional object- and style-centric manipulation, text-centric image editing focuses on modifying, translating, or rearranging textual elements embedded within images. However, existing leading models often struggle to execute complex text editing precisely, frequently producing blurry or hallucinated characters. We attribute these failures primarily to the lack of specialized training paradigms tailored for text-centric editing, as well as the absence of large-scale datasets and standardized benchmarks necessary for a closed-loop training and evaluation system. To address these limitations, we present WeEdit, a systematic solution encompassing a scalable data construction pipeline, two benchmarks, and a tailored two-stage training strategy. Specifically, we propose a novel HTML-based automatic editing pipeline, which generates 330K training pairs covering diverse editing operations and 15 languages, accompanied by standardized bilingual and multilingual benchmarks for comprehensive evaluation. On the algorithmic side, we employ glyph-guided supervised fine-tuning to inject explicit spatial and content priors, followed by a multi-objective reinforcement learning stage to align generation with instruction adherence, text clarity, and background preservation. Extensive experiments demonstrate that WeEdit outperforms previous open-source models by a clear margin across diverse editing operations.

**Date:** March 13, 2026

**Project Page:** <https://huizhang0812.github.io/WeEdit/>

## 1 Introduction

In recent years, diffusion models [24, 30, 61] have made significant progress in generative tasks, particularly in image generation and editing. Text-to-image models [25, 37, 56, 58] aim to generate high-quality, visually appealing images from textual prompts. Upon this, image editing models [14, 29, 85] have been developed to modify specific content within existing images based on instructions, while preserving non-target regions.

Currently, leading proprietary models (e.g. Gemini-3-Pro-Image [12] and GPT-Image-1.5 [8]) and open-source models (e.g. FLUX.2-dev [38] and Qwen-Image-Edit [71]) excel in general image editing, demonstrating precise adherence to user instructions for object manipulation and style transfer. However, a critical yet fundamentally distinct dimension—text-centric image editing, which involves modifying, translating, or rearranging textual elements embedded within images—remains largely underexplored. Such capabilities are important in a wide



**Figure 1 Left:** WeEdit achieves precise manipulation of textual content within images across diverse editing operations (edited regions are highlighted with blue bounding boxes). **Right:** WeEdit achieves the best performance among all open-source models on both bilingual and multilingual benchmarks, surpassing most proprietary models and ranking second only to Nano Banana Pro.

range of real-world applications, including infographic updating, poster modification, multilingual localization of user interfaces, and document editing. Unlike previous editing tasks, this task requires models to possess accurate text recognition, precise layout planning, and clear text generation abilities, all while strictly preserving the background context (as shown in figure 1).

These practical requirements expose the significant limitations of current paradigms. Existing models often struggle to follow complex editing instructions and tend to produce blurry or hallucinated characters, with performance deteriorating further when handling non-Latin scripts (e.g. Arabic, Thai, and Hindi). We attribute these failures to critical gaps in current algorithms, training data, and evaluation methodologies: **I) Algorithmic limitations:** Conventional image editing methods lacks specialized training paradigms explicitly designed to handle the unique text content modification within images. **II) Data scarcity:** There is no large-scale, high-quality datasets specifically curated for diverse text-centric editing operations, particularly for multilingual settings. **III) Evaluation gap:** The absence of a comprehensive, standardized benchmark tailored to this specific task hinders systematic model comparison, slowing down progress in this field.

To this end, we propose **WeEdit**, a systematic solution for text-centric image editing that jointly addresses the aforementioned challenges of model capability, training strategy, data scarcity, and evaluation standardization: **I) Glyph-Guided Supervised Fine-Tuning:** To tackle the core difficulty of precise text placement and character-level accuracy, we introduce a text-aware fine-tuning approach. WeEdit first predicts the approximate position and scale of the target text, then renders a glyph layout as an explicit spatial prior to condition the diffusion process, granting direct spatial control and significantly improving glyph fidelity. **II) Multi-Objective Reinforcement Learning:** To bridge the gap between pixel-level supervision and human-centric quality goals such as legibility and contextual coherence, we introduce a reinforcement learning stage with a reward function that jointly balances instruction adherence, text readability, and preservation of non-edited regions, leading to higher editing quality. **III) Scalable Data Construction Pipeline:** We develop a scalable, HTML-based data construction pipeline that automatically synthesizes diverse editing pairs. The pipeline naturally extends to multilingual settings via a “translate-then-edit” workflow, yielding a large-scale training dataset covering a broad spectrum of editing operations and languages. **IV) Standardized Multilingual Benchmark:** We establish a comprehensive benchmark encompassing diverse editing operations with both Chinese–English bilingual data and multilingual evaluation across 15 widely used languages. We further design a multi-faceted evaluation scheme to ensure practical and reliable comparisons between the models. Finally, as illustrated on the right side of figure 1, our model outperforms existing open-source models and most proprietary counterparts, achieving SOTA performance that is second only to Gemini-3-Pro-Image (i.e. Nano Banana Pro [12]).

## 2 Related Work

### 2.1 General Image Generation and Editing

Text-to-image generation [15, 20, 25–27, 37, 43, 46, 55, 56, 58, 60, 92] aims to generate visual content from textual descriptions. Image editing [14, 23, 39, 45, 72, 73, 76, 82, 85, 86, 88] extends this capability by modifying targeted regions of an existing image according to user instructions while preserving non-targeted content. Recently, leading proprietary [8, 12] and open-source models [16, 22, 38, 44, 48, 64, 65, 71], have demonstrated strong performance on object modification and style transfer. However, text-centric image editing—an equally critical yet fundamentally distinct dimension that involves modifying, translating, or rearranging textual elements embedded within images—remains largely underexplored. When confronted with such tasks, existing models frequently fail to follow editing instructions accurately and produce blurred or misspelled characters. In this paper, we aim to systematically benchmark the text-centric editing capabilities of current models and propose effective methods to bridge this gap.

### 2.2 Text-aware Image Generation and Editing

To improve text rendering quality in generated images, recent approaches incorporate additional information such as character-level linguistic features [50, 51, 90], explicit character bounding boxes [19, 83, 84, 93–95], and auxiliary visual conditions like rendered glyph images [18, 53, 66, 79, 87]. While these approaches have improved text fidelity in image generation, few have focused on the editing task. In this work, we propose to introduce glyph images as explicit spatial priors into text-centric image editing, and leveraging the understanding and planning capabilities of Vision-Language Models to automatically generate glyph images of target texts.

### 2.3 Datasets and Benchmarks for Image Editing

Existing image editing datasets [21, 33, 54, 57, 68, 69, 80, 85, 88] and benchmarks [17, 28, 48, 67, 81, 89] are primarily designed for general-purpose editing scenarios. Some works involve text-related editing tasks [54, 65], but they are limited in terms of operation diversity, language coverage, and evaluation granularity. Thus, we propose a novel automated data construction pipeline as well as the first comprehensive benchmark specifically tailored for text-centric image editing.

### 2.4 Post-training for Diffusion Models

Parameter-efficient supervised fine-tuning (SFT), such as LoRA [31], has become a mainstream approach for adapting pre-trained diffusion models to downstream tasks or for incorporating auxiliary control signals [32, 59, 63, 75]. Reinforcement learning (RL)-based [62] post-training further aligns generation with human preferences [36, 42, 47, 74, 77, 78, 91]. In this paper, we present a dedicated post-training framework for text-centric image editing, which consists of glyph-guided SFT to inject explicit visual priors, followed by a tailored reward design in the RL stage to ensure editing accuracy.

## 3 Method

In this section, we first review the preliminaries of diffusion and flow-matching models as well as the formulation of image editing (section 3.1). We then present our two-stage training framework: a glyph-guided supervised fine-tuning stage that injects explicit spatial and content priors for accurate text rendering (section 3.2), followed by a reinforcement learning stage that directly optimizes human-centric objectives such as instruction adherence, text clarity, and background preservation (section 3.3).

### 3.1 Preliminary

**Diffusion and Flow-Matching Models.** Diffusion models generate data by reversing a forward noising process that gradually corrupts clean data  $\mathbf{x}_0 \sim p_{\text{data}}$  with Gaussian noise. The noisy sample at timestep  $t$  is obtained via reparameterization:

$$\mathbf{x}_t = \alpha_t \mathbf{x}_0 + \sigma_t \boldsymbol{\epsilon}, \quad \boldsymbol{\epsilon} \sim \mathcal{N}(\mathbf{0}, \mathbf{I}), \quad (1)$$

where  $\alpha_t, \sigma_t$  define the noise schedule. Under the velocity parameterization, a neural network  $\mathbf{v}_\theta(\mathbf{x}_t, t)$  is trained to predict the trajectory tangent by minimizing:

$$\mathcal{L}_{\text{flow}} = \mathbb{E}_{t, \mathbf{x}_0, \epsilon} [\|\mathbf{v}_\theta(\mathbf{x}_t, t) - \mathbf{v}_t\|_2^2], \quad (2)$$

where  $\mathbf{v}_t = \frac{d\mathbf{x}_t}{dt} = \frac{d\alpha_t}{dt}\mathbf{x}_0 + \frac{d\sigma_t}{dt}\epsilon$ . Samples are then generated by solving the ODE  $d\mathbf{x}_t/dt = \mathbf{v}_\theta(\mathbf{x}_t, t)$  from  $t=1$  (noise) to  $t=0$  (data). Rectified flow [49] sets  $\alpha_t = 1 - t$  and  $\sigma_t = t$ , yielding straight-line interpolation paths with the simplified target  $\mathbf{v} = \epsilon - \mathbf{x}_0$ . This formulation forms the backbone of recent image editing models [38, 71]. Our framework builds upon the flow-based MM-DiT, *i.e.* Qwen-Image-Edit [71].

**Text-centric Image Editing.** Given a source image  $\mathbf{I}_{src}$  and a user-provided editing instruction  $\mathbf{p}$ , the goal of instruction-based image editing is to generate a target image  $\mathbf{I}_{tgt}$  that semantically aligns with  $\mathbf{p}$  while preserving the non-target regions of  $\mathbf{I}_{src}$ . Distinct from general object or style editing, text-centric editing requires the model to manipulate textual elements—such as modifying, translating, deleting, or rearranging text—within an image. The generated text must accurately reflect the intent of the instruction, be correctly spelled, and maintain a consistent style with the original image, while strictly preserving the integrity of the background. In this work, we focus on this practically significant dimension of image editing tasks that has not yet been fully explored.

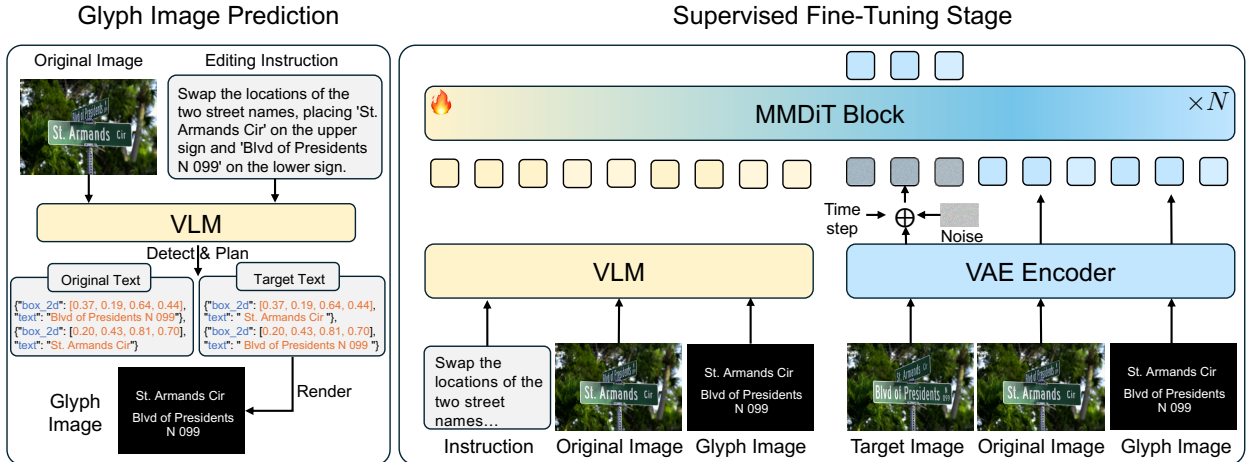


**Figure 2** Overview of the glyph-guided supervised fine-tuning stage. A VLM first predicts the content and layout of the target text to render a glyph image. The original image, instruction, and glyph image are then jointly processed by the MM-DiT block to generate the target image.

### 3.2 Supervised Fine-Tuning (SFT)

While recent diffusion models have demonstrated impressive general editing capabilities, they often struggle with complex text-centric editing scenarios such as long-text replacement or multilingual translation, frequently generating hallucinated or misplaced characters. To address this, we introduce a glyph-guided supervised fine-tuning stage to adapt a pre-trained image editing diffusion model for accurate text-centric editing. As illustrated in figure 2, our SFT pipeline comprises two key components: a glyph image prediction mechanism and a LoRA-based glyph-conditioned fine-tuning procedure.

**Glyph Image Prediction.** Given a source image  $\mathbf{I}_{src}$  and an editing instruction  $\mathbf{p}$ , we employ Qwen3-VL-235B-A22B-Instruct [13] to perform a two-step *detect-and-plan* procedure. In the detection step, the VLM identifies all text regions of interest specified by the editing instruction in the source image and outputs their bounding boxes and content as structured tuples  $\{(\mathbf{b}_i^{\text{orig}}, t_i^{\text{orig}})\}_{i=1}^m$ , where  $\mathbf{b}_i^{\text{orig}}$  denotes the normalized coordinates of the top-left and bottom-right corners, and  $t_i^{\text{orig}}$  denotes the text string. In the planning step, the VLM

interprets the editing instruction  $\mathbf{p}$  and determines the target text content and spatial placement for each region, producing the target tuples  $\{(\mathbf{b}_j^{\text{tgt}}, t_j^{\text{tgt}})\}_{j=1}^n$ . Once the layout of target texts is determined, we render the glyph image  $\mathbf{x}_{\text{glyph}}$  by drawing each target text string  $t_j^{\text{tgt}}$  within its corresponding bounding box  $\mathbf{b}_j^{\text{tgt}}$  on a blank canvas that matches the source image dimensions. To ensure high-quality and standardized glyph images, we use Python Pillow package [3] and the multilingual Arial [1] font. For simplicity, all glyph images feature white text on a black background, creating a clean and unambiguous representation of the target texts. This glyph image explicitly includes the character content, spatial positions, and relative scales of all target texts, serving as a spatial prior for the subsequent editing process.

**LoRA-based Glyph-guided Fine-tuning.** We adopt a parameter-efficient fine-tuning strategy using Low-Rank Adaptation (LoRA) [31] to train the editing model. The model takes three inputs: the editing instruction  $\mathbf{p}$ , the source image  $\mathbf{I}_{\text{src}}$ , and the glyph image  $\mathbf{I}_{\text{glyph}}$ . Specifically, the editing instruction, along with the original image and the glyph image, is first fed into the VLM to obtain semantically enriched text tokens. Meanwhile,  $\mathbf{I}_{\text{src}}$  and  $\mathbf{I}_{\text{glyph}}$  are encoded into latent representations via a VAE [35] and concatenated with the noisy latent  $\mathbf{x}_t$  along the token dimension. We keep the original weights of the MM-DiT blocks frozen, and introduce LoRA modules only into the linear layers of the multi-modal attention mechanisms. This approach enables the model to effectively incorporate information from the glyph image, maintaining low training overhead.

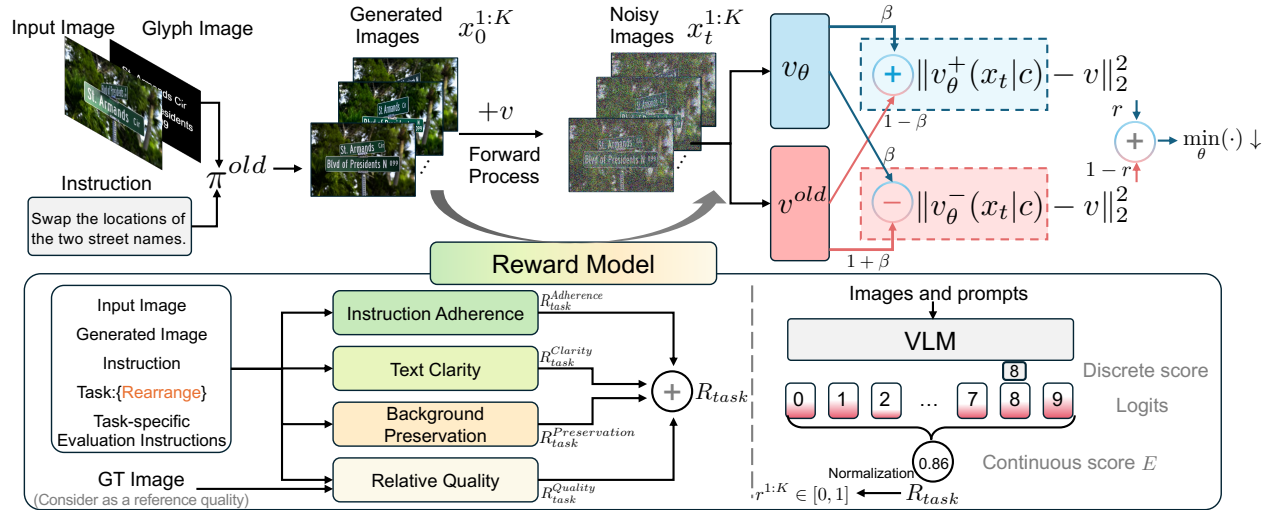


**Figure 3 Overview of the RL stage.** The model generates multiple candidate images, which are evaluated by four separate reward models targeting four dimensions. Each reward model leverages a Vision-Language Model to produce logit distributions over discrete scores, which are then converted to continuous expected values.

### 3.3 Reinforcement Learning (RL)

While the glyph-guided SFT stage equips the model with fundamental text editing capabilities, pixel-level losses cannot capture higher-level perceptual qualities such as legibility, instruction fidelity, and background coherence. To address this limitation, we introduce an RL stage that optimizes the diffusion model against a composite reward function tailored to the unique demands of text-centric image editing, as shown in figure 3.

**DiffusionNFT-based Policy Optimization.** We adopt DiffusionNFT [91] as our policy optimization framework, which performs online reinforcement learning directly on the forward diffusion process via the flow matching objective. For each conditioning input  $\mathbf{c}$  (comprising  $\mathbf{I}_{\text{src}}$ ,  $\mathbf{I}_{\text{glyph}}$ , and instruction  $\mathbf{p}$ ), we sample  $K$  candidate images  $\{\mathbf{x}_0^{1:K}\}$  from the current policy  $\pi^{\text{old}}$  using an efficient ODE solver (e.g., DPM-Solver [52]). Each candidate is then scored by the reward model to yield an optimality probability  $r \in [0, 1]$ , which serves as a soft indicator of sample quality. The training objective jointly optimizes implicitly parameterized positive and

negative policies:

$$\mathcal{L}_{\text{RL}}(\theta) = \mathbb{E}_{\mathbf{c}, \pi^{\text{old}}(\mathbf{x}_0|\mathbf{c}), t} \left[ r \|\mathbf{v}_{\theta}^+(\mathbf{x}_t, \mathbf{c}, t) - \mathbf{v}\|_2^2 + (1-r) \|\mathbf{v}_{\theta}^-(\mathbf{x}_t, \mathbf{c}, t) - \mathbf{v}\|_2^2 \right], \quad (3)$$

where  $\mathbf{v}$  denotes the target velocity, and the implicit positive and negative policies are:

$$\mathbf{v}_{\theta}^+(\mathbf{x}_t, \mathbf{c}, t) := (1 - \beta) \mathbf{v}^{\text{old}}(\mathbf{x}_t, \mathbf{c}, t) + \beta \mathbf{v}_{\theta}(\mathbf{x}_t, \mathbf{c}, t), \quad (4)$$

$$\mathbf{v}_{\theta}^-(\mathbf{x}_t, \mathbf{c}, t) := (1 + \beta) \mathbf{v}^{\text{old}}(\mathbf{x}_t, \mathbf{c}, t) - \beta \mathbf{v}_{\theta}(\mathbf{x}_t, \mathbf{c}, t). \quad (5)$$

This formulation establishes a contrastive improvement direction: the positive branch pulls the  $\mathbf{v}_{\theta}$  toward high-reward generations, while the negative branch pushes it away from low-reward ones, with the hyperparameter  $\beta$  controlling the guidance strength.

**Task-Specific Multi-Dimensional Reward.** We design a reward function specifically tailored to the multi-faceted requirements of text-centric image editing. Rather than relying on a single holistic quality score, we decompose the reward into four complementary dimensions, each targeting a critical and distinct aspect of editing quality:

**(1) Instruction Adherence** ( $R_{\text{task}}^{\text{Adherence}}$ ) evaluates whether the edited image faithfully executes the specified editing operation (e.g. whether the correct text has been replaced, translated, or rearranged at the instructed locations). We prompt Qwen3-VL-235B-A22B-Instruct [13] as a reward model (same below), which takes the original image, the edited image, and the editing instruction as input, and assesses the degree of semantic alignment between the instruction intent and the actual edit.

**(2) Text Clarity** ( $R_{\text{task}}^{\text{Clarity}}$ ) measures the legibility and typographic quality of the rendered text. The VLM evaluates whether the generated characters are crisp, correctly spelled, and free from common artifacts such as blurriness, stroke distortion, or character merging—issues that are prevalent in text-centric editing tasks involving fine-grained glyph details.

**(3) Background Preservation** ( $R_{\text{task}}^{\text{Preservation}}$ ) assesses whether non-target regions of the image remain unaltered after editing. Unintended modifications—such as color shifts, structural distortions, or texture degradation—are penalized to ensure that edits are strictly confined to the designated text regions.

**(4) Relative Quality** ( $R_{\text{task}}^{\text{Quality}}$ ) compares the overall visual quality of the edited image against a reference image, which can be either a ground-truth image or an output produced by a leading editing model. By grounding the evaluation in an explicit comparison target, this metric provides the VLM with a sharper perception of what constitutes a high-quality edit result, effectively establishing a quality anchor. As a result, the editing model is encouraged not only to produce outputs that merely appear satisfactory, but to generate edits that truly match or surpass the reference.

**Logit-Weighted Continuous Scoring.** Inspired by UniWorld-V2 [44], we adopt a logit-based continuous scoring mechanism to avoid the sparsity in single-integer reward signals. For each evaluation dimension, the VLM [13] receives an input tuple  $\mathbf{X} = (\mathbf{I}_{\text{src}}, \mathbf{I}_{\text{edited}}, T_{\text{prompt}})$ , where  $T_{\text{prompt}}$  is a dimension- and task-specific prompt instructing the VLM to rate the edit on a scale from 0 to 9. Instead of sampling a single token, we compute a softmax over the score token set  $\mathcal{S} = \{0, 1, \dots, 9\}$  at the designated decoding position and obtain the per-dimension reward as the normalized expected score:

$$R_{\text{task}}^{\text{dim}}(\mathbf{X}) = \frac{1}{\max(\mathcal{S})} \sum_{s \in \mathcal{S}} s \cdot \frac{\exp(z_s)}{\sum_{s' \in \mathcal{S}} \exp(z_{s'})}, \quad (6)$$

where  $z_s$  is the logit for score token  $s$ . This soft scoring captures the VLM’s full confidence distribution, yielding a smoother reward score. The composite reward for each candidate is a weighted sum of all four dimensions:

$$R_{\text{task}} = \lambda_{\text{acc}} R_{\text{task}}^{\text{Adherence}} + \lambda_{\text{cla}} R_{\text{task}}^{\text{Clarity}} + \lambda_{\text{pre}} R_{\text{task}}^{\text{Preservation}} + \lambda_{\text{qua}} R_{\text{task}}^{\text{Quality}}, \quad (7)$$

where  $\lambda_{\text{acc}}, \lambda_{\text{cla}}, \lambda_{\text{pre}}, \lambda_{\text{qua}}$  balance the relative importance of each dimension. Notably, the evaluation prompt for each dimension is further customized by editing task type (e.g., replace, translate, rearrange, or delete), enabling task-aware scoring criteria.

To feed  $R_{\text{task}}$  into the policy optimization process, we convert it to an optimality probability  $r \in [0, 1]$  via intra-group normalization:

$$r(\mathbf{x}_0, \mathbf{c}) = \frac{1}{2} + \frac{1}{2} \text{clip} \left[ \frac{R_{\text{task}}(\mathbf{x}_0, \mathbf{c}) - \mu_{\mathbf{c}}}{\sigma_{\mathbf{c}}}, -1, 1 \right], \quad (8)$$

where  $\mu_{\mathbf{c}}$  and  $\sigma_{\mathbf{c}}$  are the mean and standard deviation of  $R_{\text{task}}$  over the  $K$  candidates sampled for conditioning input  $\mathbf{c}$ . This normalization ensures that  $r$  reflects relative quality within each sample group. The value of  $r$  is then used to directly weight the positive and negative branches in  $\mathcal{L}_{\text{RL}}$ .

## 4 Dataset and Benchmark

In this section, we first introduce our data construction pipeline, which generates high-quality source–target image pairs via two complementary routes (Sec. 4.1). We then introduce our evaluation benchmark, covering bilingual (Chinese–English) and multilingual (15 languages) text-centric editing scenarios (Sec. 4.3).

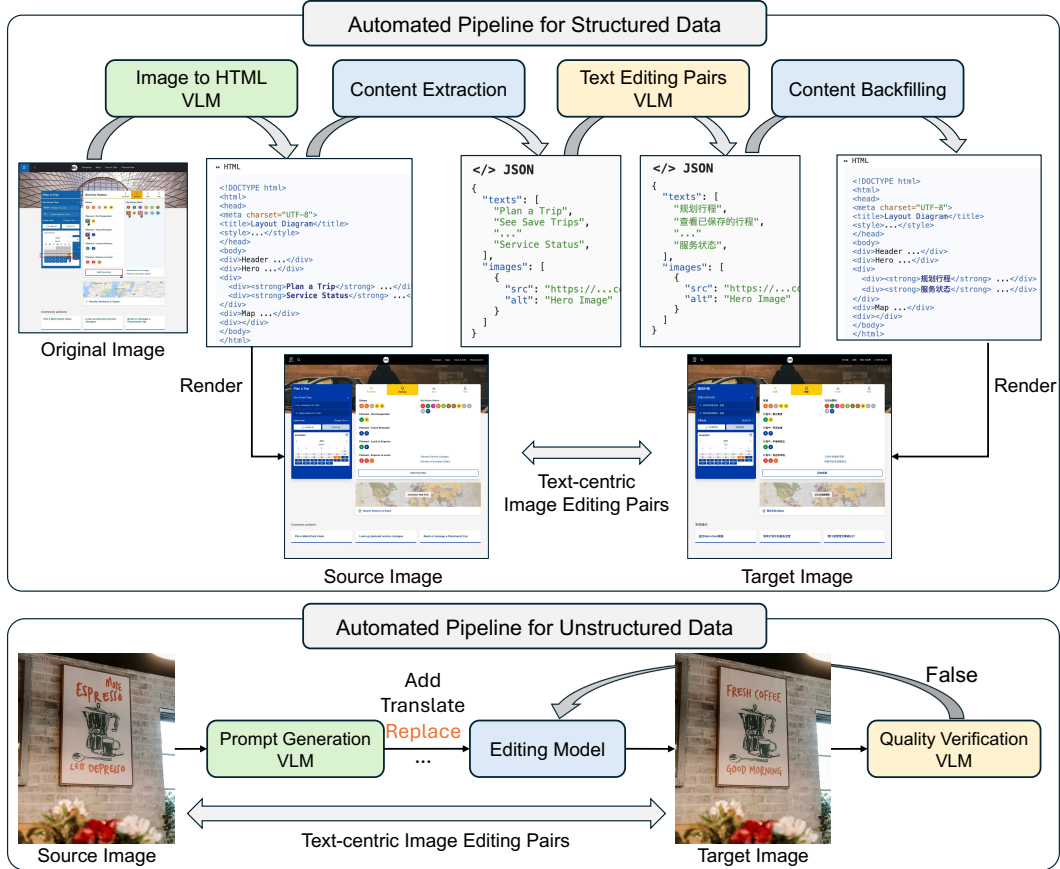


**Figure 4** Overview of our data construction pipelines. **Top:** the structured pipeline converts a source image to HTML, extracts and edits text content via a VLM, and renders both source and target images through a headless browser, yielding pixel-perfect editing pairs. **Bottom:** the unstructured pipeline uses a VLM to propose editing instructions, executes edits with a generative model, and iteratively verifies quality until all acceptance criteria are met.

## 4.1 Dataset

Our dataset is designed to cover a broad spectrum of text-centric editing tasks. We define 7 operation types: Add (inserting new text), Replace (substituting existing text with different content), Delete (removing text regions), Rearrange (permuting the spatial layout of text elements), Translate (converting text between languages), Change Style (modifying font, color, or typographic attributes), and Combined (composing multiple atomic operations in a single instruction). Based on the nature of the source images, we identified two fundamentally different data categories—structured and unstructured—and designed a dedicated construction process for each, as illustrated in [figure 4](#).

**Structured Data.** For images with well-organized layouts and relatively uniform text styles—such as web page screenshots, mobile app interfaces, presentation slides, figures, tables, documents, and infographics—we adopt a novel HTML-based construction pipeline ([figure 4](#), top). We collected a wide range of source images from various open-source datasets, including Leopard [34], The Cauldron [40], WebSight [41], etc. The pipeline proceeds in four stages:

**(1) Image to HTML.** Given an original image  $\mathbf{I}_{\text{ori}}$ , we employ a VLM [11] to convert it into an HTML representation  $\mathcal{H}_{\text{src}}$  that preserves both the visual layout and the textual content as faithfully as possible, using Tailwind [5] CSS for styling.

**(2) Content Extraction.** We use BeautifulSoup4 [2] to parse  $\mathcal{H}_{\text{src}}$  and extract a structured JSON record containing all text elements and image elements. For images, we validate external URLs and retrieve semantically similar replacements from the web when the original links are broken, ensuring rendering fidelity.

**(3) Text Editing Pairs.** Given the  $N$  text entries extracted from  $\mathcal{H}_{\text{src}}$ , we employ a lightweight VLM Qwen3-30B-A3B [13] to generate the corresponding edited texts for each operation type. Specifically, for translation, all  $N$  entries are translated into the target language; for replacement, 1 to  $N$  entries are randomly selected, and the VLM produces semantically plausible substitutes.

**(4) Content Backfilling.** Once the target texts are determined, we substitute them into  $\mathcal{H}_{\text{src}}$  at exactly the positions of the original text entries, leaving all other HTML elements unchanged, thereby producing the modified HTML code  $\mathcal{H}_{\text{tgt}}$ .

**(5) Rendering.** Both  $\mathcal{H}_{\text{src}}$  and  $\mathcal{H}_{\text{tgt}}$  are rendered into images via Playwright [4]. As the rendering process is fully deterministic and  $\mathcal{H}_{\text{src}}$  and  $\mathcal{H}_{\text{tgt}}$  differ only in the designated text entries, the resulting source image  $\mathbf{I}_{\text{src}}$  and target image  $\mathbf{I}_{\text{tgt}}$  are guaranteed to be pixel-perfect identical in all non-target regions.

Another key advantage of our HTML-based pipeline is its natural extensibility to multilingual data. Before constructing editing pairs, we can first translate all text entries in  $\mathcal{H}_{\text{src}}$  into a target language to obtain a multilingual-based HTML, and then apply the same pair-construction workflow on top of it. In this work, we cover 15 widely used languages: English, Chinese, Hindi, Spanish, French, Arabic, Portuguese, Bengali, Russian, German, Korean, Japanese, Thai, Indonesian, and Vietnamese. Through this automated HTML-based pipeline, we efficiently construct large-scale, high-quality, and linguistically diverse text-centric editing pairs.

**Unstructured Data.** For images with complex layouts, diverse typography, and text is tightly entangled with complex visual backgrounds (e.g., street signs, product packaging, posters, and scene photographs), HTML-based reconstruction cannot faithfully recover the intricate visual styles. To address this, we develop an automated edit-verify-and-retry pipeline that operates directly at the image level ([figure 4](#), bottom). Given a source image  $\mathbf{I}_{\text{src}}$ , a VLM [11] first analyzes its content and proposes a set of plausible editing instructions covering various task types. Each instruction is then executed by an editing model [12, 38, 71] to produce a candidate target image  $\hat{\mathbf{I}}_{\text{tgt}}$ . A separate VLM-based [11] verifier evaluates the candidate against the source image and instruction on instruction adherence, text legibility, and background preservation. Failed candidates are fed back with verification feedback for re-execution; only candidates passing all checks are retained as valid training pairs. This closed-loop workflow ensures high data quality for visually challenging scenes and naturally filters out ambiguous or infeasible edits, producing a clean and diverse complement to the structured data.

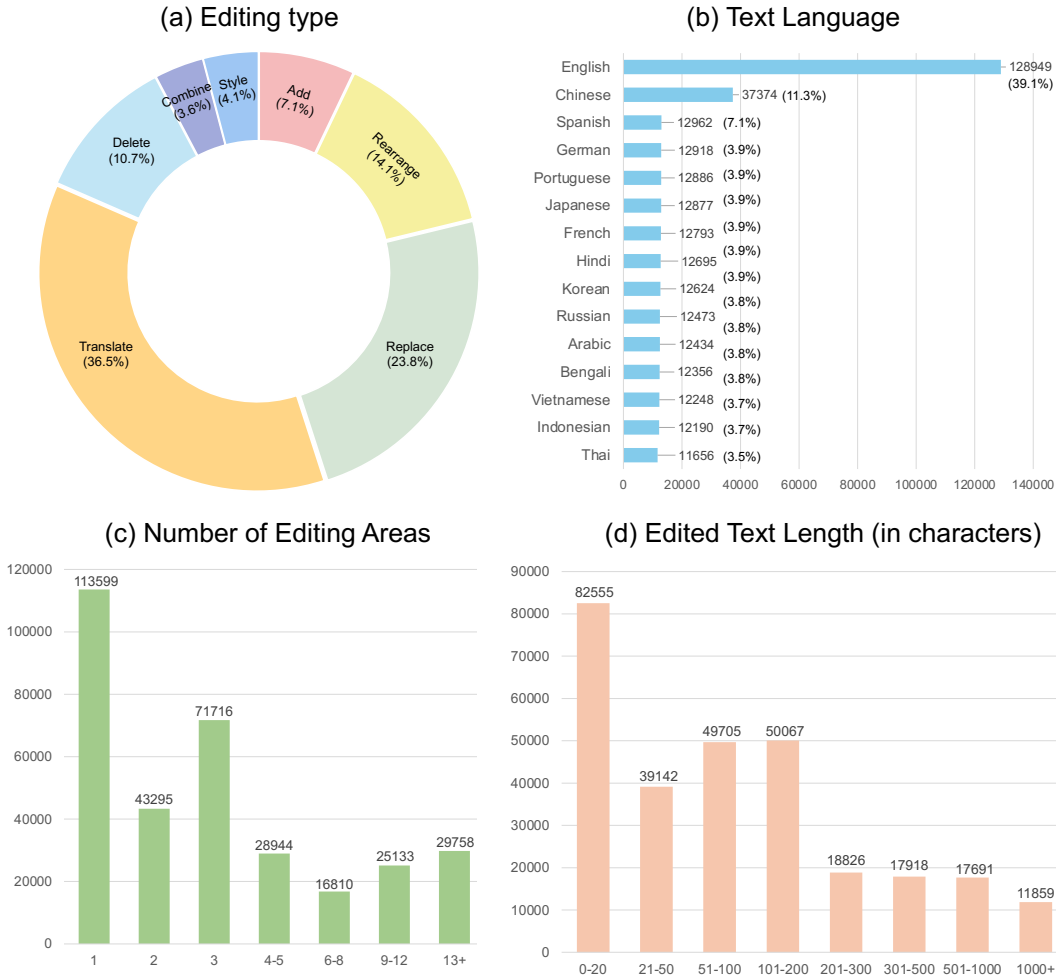


**Figure 5** Statistics of WeEdit Dataset: (a) Distribution over the seven editing operation types. (b) Language distribution across 15 supported languages. (c) Distribution of the number of edited regions per sample. (d) Distribution of the total edited text length (in characters) per sample.

## 4.2 Statistics of Datasets

We construct a training set containing 330K samples, including approximately 160K unstructured text pairs and 170K structured text pairs. The dataset spans 7 editing operation types and covers 15 languages. As shown in [figure 5\(a\)](#), translation (36.5%) and replacement (23.8%) together account for over 60% of all samples, reflecting their prevalence in real-world text editing scenarios. Rearrange (14.1%) and delete (10.7%) operations also constitute substantial portions, while add (7.1%), style change (4.1%), and combined editing (3.6%) provide complementary coverage of less frequent but practically important operations. [figure 5\(b\)](#) illustrates the language distribution. Although English (39.1%) and Chinese (11.3%) dominate due to their abundance in existing corpora, we intentionally balance the remaining 13 languages—including Spanish, German, Portuguese, Japanese, French, Hindi, Korean, Russian, Arabic, Bengali, Vietnamese, Indonesian, and Thai—to each comprise approximately 3.5%–7.1% of the dataset, ensuring broad multilingual coverage. In terms of editing complexity, [figure 5\(c\)](#) shows that single-region edits are the most common (113,599 samples), yet a significant proportion of samples involve multi-region editing: over 100K samples require editing two or more regions simultaneously, and nearly 30K samples involve 13 or more regions. This distribution encourages the model to learn both precise localized edits and coordinated multi-region modifications. Finally, [figure 5\(d\)](#) reveals a wide spread in edited text length. While short edits (0–20 characters) are the most frequent (82,555 samples), a long tail extends to over 1,000 characters (11,859 samples), covering scenarios from brief label

modifications to full paragraph-level rewrites. This diversity in both region count and text length ensures that our dataset comprehensively captures the complexity spectrum of real-world text image editing tasks.

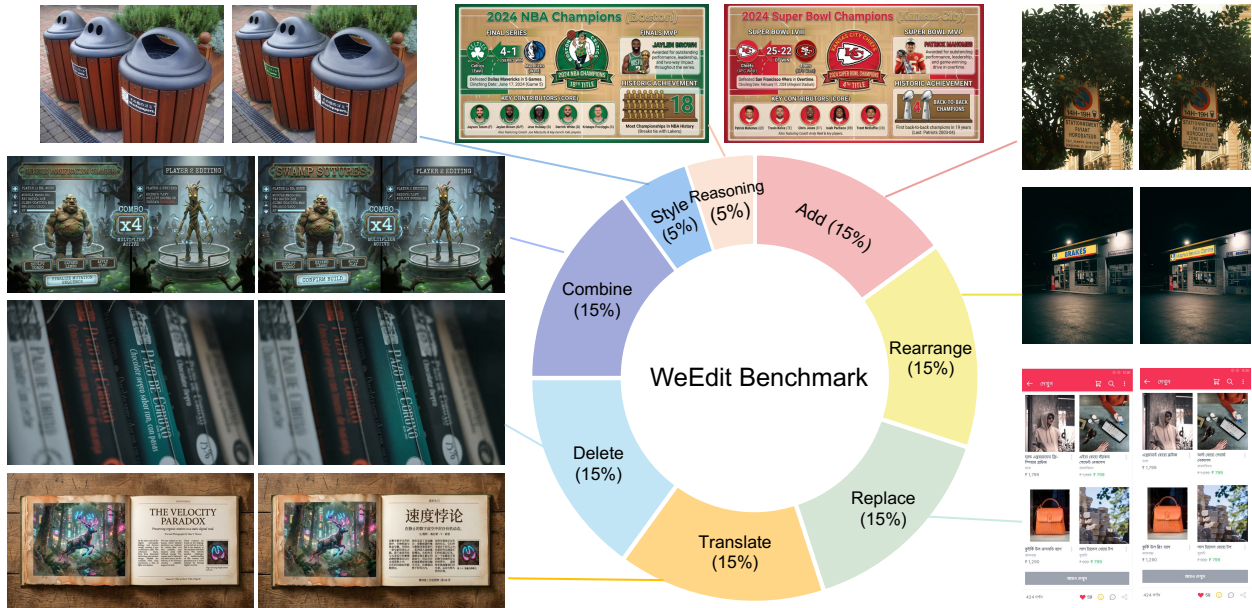


Figure 6 Overview of the proposed WeEdit Benchmark.

### 4.3 Benchmark

As illustrated in figure 6, we construct a comprehensive benchmark that covers a diverse set of text-centric editing operations, supports multiple languages, and evaluates model performance along three complementary dimensions.

**Diverse Editing Operations.** Our benchmark encompasses eight distinct task categories to thoroughly assess model capabilities. Six of these focus on direct textual content manipulation: *Add*, *Replace*, *Delete*, *Rearrange*, *Translate*, and *Combined* (executing multiple atomic operations simultaneously). Furthermore, we include *Change Style* to evaluate the modification of typographic attributes (e.g., font, color). In addition, we introduce a more advanced *Reasoning* task that goes beyond the operation types found in the training set. This task requires the model to first deduce the correct target text based on knowledge or logical context before performing the edit. For instance, replacing “2024 NBA Champions (Boston)” with “2024 Super Bowl Champions” requires the model to recall relevant factual knowledge (e.g., team names, scores, and player details) to obtain the target text content before editing.

**Comprehensive Language Coverage.** To evaluate the robustness of editing models across different linguistic contexts, the benchmark is provided in two distinct versions, each containing 2,000 test cases. The *Bilingual Benchmark* focuses on Chinese and English, representing typical high-frequency scenarios. Meanwhile, the *Multilingual Benchmark* extends the evaluation to 15 widely used languages, testing the models’ generalization ability to diverse character sets and complex glyph structures.

**Evaluation Metrics.** We adopt a VLM-based automatic evaluation protocol, employing Gemini-3-Pro [11] as an impartial judge to score generated images across three core dimensions: *Instruction Adherence* (IA), which measures the degree to which the edited image faithfully fulfills each requirement specified in the editing instruction; *Text Clarity* (TC), which assesses the legibility and spelling correctness of the generated text; and *Background Preservation* (BP), which quantifies the visual integrity of non-target regions. The judge is prompted to first generate a detailed chain-of-thought [70] rationale that examines the edited image

against the evaluation criterion, and then assign a score on a 0–9 scale, thereby producing fine-grained quality assessments.

## 5 Experiment

### 5.1 Experimental Setup

**Dataset and Evaluation Metrics.** We train our models on the proposed WeEdit dataset. For evaluation, we utilize the WeEdit Benchmark, consisting of a Bilingual Benchmark (Chinese and English) and a Multilingual Benchmark, each containing 2,000 meticulously curated test cases to thoroughly assess model capabilities. Following section 4.3, we employ Gemini-3-Pro [11] to assess the edited images from three dimensions.

**Implementation Details.** During the SFT stage, we fine-tune Qwen-Image-Edit-2509 [9] using LoRA with a rank of 256. The model is optimized with AdamW at a learning rate of 5e-5, trained for 8,000 steps. In the RL stage, the model is initialized with the SFT weights and further fine-tuned using LoRA (rank 256) and AdamW with the same learning rate. Training is conducted for 140 epochs.

### 5.2 Main Results

**Baseline Methods.** To comprehensively evaluate our proposed WeEdit framework, we compare it against 15 previous SOTA baselines, including 4 prominent proprietary models [6–8, 12] and 11 leading open-source models [9, 10, 16, 22, 23, 38, 44, 48, 64, 65, 72]. The evaluation is conducted on both our Bilingual and Multilingual benchmarks, systematically covering 8 diverse editing operations. For each operation, the edited images are rigorously assessed across three complementary criteria: Instruction Adherence (IA), Text Clarity (TC), and Background Preservation (BP).

Model	Add			Replace			Delete			Rearrange			Translate			Style			Combined			Reasoning			Overall		
	IA	TC	BP																								
Gemini-3-Pro-Image [12]	<b>9.38</b>	<b>9.66</b>	<b>9.43</b>	<b>9.06</b>	<b>8.80</b>	<b>8.05</b>	<b>8.33</b>	<b>8.56</b>	<b>8.04</b>	<b>8.05</b>	<b>8.49</b>	<b>8.26</b>	<b>8.08</b>	<b>9.07</b>	<b>9.55</b>	<b>9.76</b>	9.51	<b>9.50</b>	<b>9.31</b>	<b>9.72</b>	<b>9.45</b>	<b>4.91</b>	<b>9.47</b>	<b>9.42</b>	<b>8.58</b>	<b>9.10</b>	<b>8.85</b>
Gemini-2.5-Flash-Image [7]	5.88	8.06	7.58	3.35	6.05	7.50	6.01	8.17	6.05	1.77	6.86	7.11	1.75	6.06	8.83	7.95	<b>9.54</b>	9.58	4.08	7.57	8.83	1.70	4.82	8.76	3.92	7.14	7.80
GPT-Image-1.5 [8]	8.02	9.32	6.80	7.16	7.58	5.55	6.43	6.49	3.82	5.44	6.91	5.35	4.09	6.97	7.71	9.30	9.44	8.31	8.12	9.12	6.34	3.37	7.02	7.93	6.52	7.78	6.15
Seedream4.5 [6]	6.86	8.21	6.40	7.23	7.93	5.91	6.60	7.37	4.70	5.29	7.08	5.36	4.97	6.93	7.15	8.76	9.08	8.37	7.33	8.62	7.66	2.17	5.69	7.67	6.29	7.66	6.38
OmniGen2 [72]	1.72	3.11	3.86	1.26	3.30	3.61	1.53	3.54	2.52	1.07	3.34	3.32	1.00	3.35	3.85	3.67	5.29	4.21	1.21	3.41	3.92	1.01	4.15	6.24	1.40	3.48	3.68
BAGEL [23]	2.32	3.03	5.99	1.48	2.41	4.30	3.03	6.46	2.92	1.07	3.53	5.66	1.03	4.88	7.68	7.36	7.76	8.98	1.44	2.33	5.83	1.02	4.42	8.89	1.97	4.01	5.75
Emu3.5 [22]	4.89	6.60	3.72	3.26	4.60	2.81	4.76	5.20	2.29	1.46	3.94	3.36	1.27	2.73	5.93	8.27	8.66	8.41	3.96	5.98	4.13	1.23	3.34	6.32	3.42	4.96	4.07
UniWorld-v2 [44]	5.15	7.16	5.41	3.27	5.06	4.29	4.23	7.13	2.88	1.47	4.33	4.39	1.32	2.36	8.50	8.78	8.98	8.55	3.52	6.22	5.08	1.22	4.10	7.97	3.34	5.49	5.41
FLUX.2-dev [38]	5.40	7.59	4.92	3.59	6.09	4.95	3.07	8.14	5.27	1.44	5.73	5.84	1.24	3.59	8.78	8.04	8.88	8.31	4.60	7.31	5.52	1.26	<b>6.33</b>	<b>9.55</b>	3.37	6.53	6.19
Qwen-Image-Edit-2511 [10]	4.80	5.94	3.73	3.36	3.73	3.77	3.89	4.46	3.34	1.42	2.67	3.95	1.28	1.60	6.97	8.50	8.88	8.48	3.27	4.21	4.23	1.09	1.97	6.04	3.18	3.93	4.63
LongCat-Image-Edit [64]	5.23	6.10	6.80	3.03	4.51	5.16	4.65	7.18	5.84	1.33	4.91	5.92	1.29	4.42	8.29	8.40	8.95	9.27	3.89	5.47	6.87	1.17	5.05	8.38	3.39	5.59	6.71
Step1X-Edit-v1.2 [48]	2.73	3.98	7.38	2.44	3.22	6.75	5.68	7.01	6.45	1.26	3.46	4.76	1.34	2.84	7.64	7.78	8.54	8.67	2.12	3.79	7.89	1.09	5.81	9.37	2.78	4.36	7.03
HY-image-3-instruct [16]	6.04	7.55	7.68	3.91	5.42	5.79	6.32	7.85	4.69	1.73	4.26	6.59	1.45	3.52	8.67	<b>9.43</b>	<b>9.35</b>	9.52	4.73	6.62	7.43	1.12	4.67	8.65	4.16	5.99	7.03
FireRed-Image-Edit [65]	5.44	7.54	7.67	4.58	6.30	6.26	6.80	8.81	5.97	1.76	4.78	5.52	1.39	2.67	8.44	9.30	9.23	<b>9.78</b>	4.19	7.23	7.48	1.25	5.45	8.90	4.15	6.33	7.14
Qwen-Image-Edit-2509 [9]	4.96	7.05	6.55	3.44	5.17	5.90	4.97	7.84	5.07	1.35	4.90	5.91	1.26	2.72	8.77	8.97	9.15	9.11	3.90	6.48	7.24	1.22	5.17	8.51	3.49	5.84	6.80
<b>WeEdit-SFT (ours)</b>	7.83	8.54	9.18	6.36	6.75	7.76	<b>9.28</b>	9.12	<b>8.43</b>	7.06	7.18	8.50	5.14	5.24	8.72	8.87	8.54	8.94	7.28	8.35	9.14	2.08	2.48	8.56	6.99	7.33	8.63
<b>WeEdit-RL (ours)</b>	<b>8.12</b>	<b>8.99</b>	<b>9.40</b>	<b>6.90</b>	<b>7.77</b>	<b>8.63</b>	8.92	<b>9.49</b>	8.09	<b>7.82</b>	<b>7.94</b>	<b>9.00</b>	<b>6.36</b>	<b>7.11</b>	<b>9.44</b>	9.41	9.24	9.47	<b>7.50</b>	<b>8.89</b>	<b>9.38</b>	<b>2.57</b>	5.24	8.99	<b>7.47</b>	<b>8.19</b>	<b>9.01</b>
<i>vs. Baseline</i>	+3.16	+1.94	+2.85	+3.46	+2.6	+2.73	+3.95	+1.65	+3.02	+6.47	+3.04	+3.09	+5.10	+4.39	+0.67	+0.44	+0.09	+0.36	+3.6	+2.41	+2.14	+1.35	+0.07	+0.48	+3.98	+2.35	+2.21

**Table 1 Quantitative Results on the Bilingual Benchmark.** We compare WeEdit with proprietary and open-source models across 8 editing operations. IA, TC, and BP denote Instruction Adherence, Text Clarity, and Background Preservation. The best open-source results are in **bold**, with top-3 highlighted. Our method significantly improves text editing over the base model, outperforms all open-source models, and surpasses most proprietary systems.

**Quantitative Comparison.** table 1 and table 2 present results on the Bilingual and Multilingual benchmarks, respectively. We observe that text-centric image editing remains a fundamental weakness of existing proprietary and, in particular, open-source models. On the Bilingual benchmark, the best-performing open-source baseline achieves only 4.16 overall IA, and the situation deteriorates further on more challenging tasks: on Rearrange and Translate, all open-source baselines score below 1.8 IA, indicating near-complete failure. Even strong proprietary systems (e.g. GPT-Image-1.5 and Seedream4.5) exhibit quality degradation on these tasks, confirming that text-centric editing poses challenges qualitatively different from conventional object or style editing. WeEdit establishes a new SOTA among open-source models by a clear margin and is surpassed only

by the proprietary Gemini-3-Pro-Image. On the Bilingual benchmark, our RL version (WeEdit-RL) achieves 7.47/8.19/9.01 in IA/TC/BP, improving over the base model by +3.98/+2.35/+2.21 and surpassing the previous best open-source results by a clear margin. The gains are more pronounced in tasks such as Translate and Rearrange. Moreover, WeEdit demonstrates top-tier performance across all other editing operations.

Model	Add			Replace			Delete			Rearrange			Translate			Style			Combined			Reasoning			Overall		
	IA	TC	BP																								
Gemini-3-Pro-Image [12]	<b>9.59</b>	<b>9.35</b>	<b>8.83</b>	<b>8.39</b>	<b>8.21</b>	6.97	<b>8.17</b>	<b>8.08</b>	<b>6.71</b>	<b>7.37</b>	<b>7.97</b>	<b>7.11</b>	<b>6.34</b>	<b>7.60</b>	8.66	<b>8.82</b>	<b>8.77</b>	7.78	<b>8.83</b>	<b>8.77</b>	8.12	<b>6.04</b>	<b>8.87</b>	<b>9.29</b>	<b>8.05</b>	<b>8.38</b>	7.82
Gemini-2.5-Flash-Image [7]	6.23	8.12	8.49	3.25	6.42	<b>7.56</b>	6.31	8.06	6.32	1.84	6.67	7.09	1.83	5.28	<b>8.80</b>	6.74	8.68	<b>8.76</b>	5.07	7.74	<b>8.94</b>	1.75	4.08	8.67	4.11	6.99	<b>7.95</b>
GPT-Image-1.5 [8]	7.75	8.65	3.16	5.37	6.34	3.29	5.34	4.36	1.72	4.29	5.61	3.21	2.97	5.75	5.54	6.50	7.37	3.34	7.54	7.70	3.04	2.51	4.47	5.09	5.44	6.34	3.41
Seedream4.5 [6]	6.33	7.56	5.88	5.01	6.14	5.17	6.25	6.51	4.23	3.82	5.61	4.37	3.04	5.14	6.53	7.27	8.07	6.22	6.51	7.73	6.42	1.85	4.55	7.49	5.10	6.43	5.56
OmniGen2 [72]	1.71	2.74	3.04	1.13	2.93	2.68	1.75	3.48	2.08	1.07	3.38	2.58	1.10	3.70	4.49	2.66	4.19	2.83	1.70	3.89	3.32	1.00	4.22	5.59	1.45	3.44	3.15
BAGEL [23]	2.74	3.63	8.37	1.42	2.98	4.90	3.37	5.53	3.00	1.10	3.33	4.51	1.09	3.56	6.01	5.49	6.31	7.72	3.27	4.46	6.80	1.02	4.75	7.20	2.27	4.08	5.78
Emu3.5 [22]	5.69	7.03	3.16	2.99	4.04	2.50	4.88	4.18	1.91	1.36	3.36	2.14	1.47	2.96	4.95	5.51	6.00	3.96	5.76	6.36	3.31	1.12	1.82	3.81	3.68	4.60	3.06
UniWorld-v2 [44]	5.03	6.98	5.94	2.51	4.00	3.86	4.11	5.59	2.25	1.30	3.55	2.90	1.36	2.86	6.15	5.63	6.41	5.26	4.62	6.03	4.96	1.13	3.35	7.62	3.18	4.84	4.55
FLUX.2-dev [38]	5.86	7.66	8.38	3.53	5.79	5.27	3.43	8.01	4.68	1.42	<b>6.03</b>	5.58	1.40	<b>3.97</b>	7.88	5.90	7.68	6.26	4.82	6.46	4.75	<b>1.34</b>	<b>5.63</b>	<b>9.12</b>	3.42	6.36	6.26
Qwen-Image-Edit-2511 [10]	5.51	7.41	8.05	3.11	4.75	6.17	5.90	7.44	5.65	1.54	4.32	5.70	1.56	2.92	8.28	6.51	7.44	8.02	5.24	6.92	7.50	1.19	4.64	8.83	3.81	5.67	7.04
LongCat-Image-Edit [64]	5.48	6.40	7.21	2.83	4.46	5.13	5.06	6.68	5.22	1.35	4.78	5.32	1.36	3.68	7.54	6.95	7.39	7.87	5.76	6.59	6.95	1.09	5.34	7.80	3.68	5.52	6.39
Step1X-Edit-v1.2 [48]	2.29	5.31	8.56	1.31	3.92	5.53	4.97	6.97	5.05	1.24	3.62	4.61	1.09	3.04	6.88	4.41	6.02	6.26	2.35	5.22	6.55	1.12	5.26	7.97	2.26	4.77	6.29
HY-image-3-instruct [16]	8.19	<b>8.80</b>	8.72	4.33	5.83	6.50	6.88	7.92	<b>5.82</b>	1.64	5.35	7.06	1.75	3.88	8.66	<b>8.05</b>	<b>8.36</b>	8.20	7.78	<b>8.36</b>	8.13	1.17	4.82	8.72	5.03	6.67	7.58
FireRed-Image-Edit [65]	5.52	7.42	8.18	3.25	5.02	6.53	6.57	8.27	5.52	1.71	4.91	5.98	1.62	3.78	8.47	7.69	7.78	8.31	5.86	7.26	8.13	1.20	5.09	9.00	4.12	6.14	7.29
Qwen-Image-Edit-2509 [9]	5.35	7.09	7.03	2.88	4.83	6.08	5.46	7.12	4.85	1.39	4.77	5.39	1.44	3.70	8.26	6.96	7.73	7.45	5.01	7.02	7.49	1.16	5.13	8.60	3.63	5.82	6.67
<b>WeEdit-SFT (ours)</b>	8.29	8.50	<b>9.25</b>	5.52	6.08	8.33	<b>8.60</b>	<b>8.87</b>	<b>8.17</b>	<b>5.72</b>	<b>6.63</b>	8.07	3.92	4.08	<b>8.77</b>	7.98	8.05	<b>8.90</b>	7.72	7.71	8.82	1.80	4.88	8.55	6.46	6.98	<b>8.58</b>
<b>WeEdit-RL (ours)</b>	<b>8.47</b>	8.33	8.65	<b>6.12</b>	<b>6.30</b>	<b>8.45</b>	8.21	8.76	7.92	5.58	6.32	<b>8.10</b>	<b>5.13</b>	<b>5.18</b>	8.50	7.14	8.15	8.62	<b>8.15</b>	7.61	<b>9.16</b>	<b>2.54</b>	5.25	8.63	<b>6.70</b>	<b>7.10</b>	8.49
<i>vs. Baseline</i>	<b>+3.12</b>	<b>+1.24</b>	<b>+1.62</b>	<b>+3.24</b>	<b>+1.47</b>	<b>+2.37</b>	<b>+2.75</b>	<b>+1.64</b>	<b>+3.07</b>	<b>+4.19</b>	<b>+1.55</b>	<b>+2.71</b>	<b>+3.69</b>	<b>+1.48</b>	<b>+0.24</b>	<b>+0.18</b>	<b>+0.42</b>	<b>+1.17</b>	<b>+3.14</b>	<b>+0.59</b>	<b>+1.67</b>	<b>+1.38</b>	<b>+0.12</b>	<b>+0.03</b>	<b>+3.07</b>	<b>+1.28</b>	<b>+1.82</b>

**Table 2** Quantitative Results on the Multilingual Benchmark.

The Multilingual benchmark (table 2) further reveals that WeEdit generalizes robustly to 15 diverse languages, including those with complex glyph systems such as Arabic, Thai, and Hindi. Our model achieves 6.70/7.10/8.49 overall, improving over the base model by +3.07/+1.28/+1.82. In contrast, several proprietary and open-source models suffer performance degradation when handling non-Latin scripts. This cross-lingual robustness can be attributed to our HTML-based data construction pipeline, which naturally scales to multilingual training data.

Finally, comparing WeEdit-SFT and WeEdit-RL reveals that the RL stage provides consistent and targeted improvements. On the Bilingual benchmark, the RL stage lifts overall IA from 6.99 to 7.47 and TC from 7.33 to 8.19. This confirms that the multi-dimensional reward design effectively steers the model toward higher editing quality beyond what pixel-level supervision alone can achieve.

## 6 Experimental Results

### 6.1 More Qualitative Results

We conduct a detailed qualitative comparisons of WeEdit against six representative methods—Gemini-3-pro-Image, GPT-Image-1.5, FLUX.2-dev, Qwen-Image-Edit-2509, FireRed-Image-Edit, and Step1X-Edit-v1.2—across eight editing operation types in figures 8 to 14. We annotate three common failure modes: **red** boxes for inaccurate instruction execution, **purple** boxes for unclear or illegible rendered text, and **orange** boxes for unintended modifications to non-edited regions. Several key observations emerge from these comparisons. **First**, existing methods frequently fail to execute all sub-instructions faithfully, particularly when multiple editing operations are specified simultaneously. For instance, in the *add* task (figure 8), most baselines omit at least one of the four required additions, whereas WeEdit accurately places all specified text elements at the correct locations. **Second**, text clarity remains a significant challenge for open-source models. As shown in the *replace* (figure 9) and *translate* (figure 11) examples, methods such as FireRed-Image-Edit and Step1X-Edit-v1.2 frequently produce blurry or garbled characters, especially for non-Latin scripts (e.g. Chinese). In contrast, WeEdit consistently renders sharp and legible text across all languages. **Third**, background preservation is a persistent weakness of existing approaches. Both proprietary models (e.g., GPT-Image-1.5) and open-source methods (e.g., FLUX.2-dev) often introduce noticeable artifacts or alter the visual appearance of non-edited regions, as evident in the *delete* and *style change* tasks (figures 10 and 12). WeEdit, benefiting from its task-aware reward design that explicitly penalizes background degradation, maintains high fidelity in unedited areas. **Fourth**, for complex operations such as *rearrange* (figure 10), *combined editing* (figure 13), and

*reasoning-based editing* (figure 14), most baselines either misinterpret the spatial semantics of the instruction or fail to produce logically coherent content. These results collectively demonstrate that WeEdit achieves superior performance in instruction adherence, text clarity, background preservation, and semantic reasoning across diverse editing scenarios.

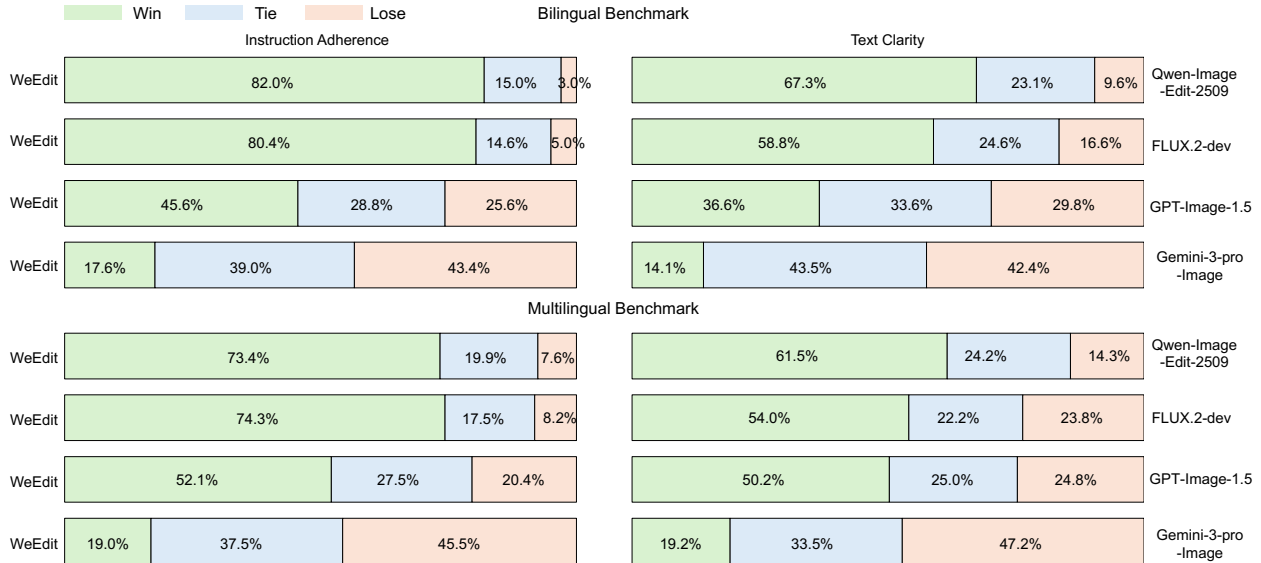


Figure 7 User Study.

**User Study.** To subjectively evaluate the editing quality, we conducted a user study comparing WeEdit against two open-source models and two proprietary systems. As illustrated in figure 7, human evaluators assessed the generated results across two dimensions: Instruction Adherence and Text Clarity on both Bilingual and Multilingual benchmarks. The results demonstrate that WeEdit significantly outperforms the open-source baselines Qwen-Image-Edit-2509 and FLUX.2-dev, as well as the proprietary GPT-Image-1.5, while achieving comparable performance with Gemini-3-Pro-Image.

Ablation					Performance		
SFT	Glyph	RL	RI	SRM	IA	TC	BP
					3.49	5.84	6.80
	✓				3.58	4.67	6.82
✓					5.32	6.62	8.11
✓		✓	✓	✓	5.41	6.72	8.07
✓	✓				6.99	7.33	8.63
✓	✓	✓		✓	7.38	7.91	8.92
✓	✓	✓	✓		7.34	8.03	8.89
✓	✓	✓	✓	✓	<b>7.47</b>	<b>8.19</b>	<b>9.01</b>

Table 3 Ablation study on different modules in WeEdit.

## 6.2 Ablation Study

To systematically evaluate the contribution of each proposed module in WeEdit, we conduct a comprehensive ablation study, as summarized in table 3. As shown in the first row, the base model exhibits poor performance across three dimensions. Applying glyph guidance directly to the baseline model at the inference stage (Row

2) results in negligible performance changes, indicating that the base model cannot effectively incorporate explicit spatial priors without specific training. Comparing the baseline with the SFT-only model (Row 3) reveals a significant performance leap across all three dimensions, which demonstrates the high quality and effectiveness of our constructed dataset. Furthermore, introducing RL directly on top of this SFT-only baseline (Row 4) struggles to break through to a higher performance ceiling. In contrast, combining SFT with Glyph guidance (Row 5) yields massive improvements, demonstrating a strong synergy where SFT aligns the model with the task while the Glyph prior provides the crucial spatial constraints needed for precise text rendering. Building upon this foundation, applying RL on top of the SFT-with-glyph model leads to further consistent enhancements. Within the RL stage, the design of the reward mechanism proves critical. Removing the Reference Image (RI) deprives the reward model of an explicit comparison anchor (Row 6), resulting in less accurate assessment of edit quality than when the reference is included. Relying on a single reward model to score multiple dimensions simultaneously leads to sub-optimal performance due to metric entanglement (Row 7), whereas using Separate Reward Models (SRM) ensures the independent and accurate assessment of each dimension. Ultimately, the full WeEdit pipeline (Row 8) achieves the best performance across all metrics, validating the necessity and effectiveness of our proposed training strategies and data.

## 7 Conclusion

In this paper, we presented WeEdit, a systematic solution for text-centric image editing that jointly addresses the challenges of model capability, data scarcity, and evaluation standardization. We introduced a glyph-guided supervised fine-tuning approach that leverages rendered glyph images as explicit spatial priors to enable precise text placement and character-level fidelity. We further proposed a multi-objective reinforcement learning stage with separate reward models and reference image grounding to optimize for instruction adherence, text readability, and background preservation. To overcome the lack of high-quality training data, we proposed a novel, scalable, HTML-based data construction pipeline that automatically synthesizes diverse editing pairs and naturally extends to multilingual settings. Additionally, we established a comprehensive benchmark covering diverse editing operations with bilingual and multilingual evaluation across 15 languages. Extensive experiments demonstrated that WeEdit surpasses existing open-source models and most proprietary counterparts.

- 1) Add 'The journey of the metal is the journey of the self.' below the existing paragraphs on the left, 2) Add a label 'Polished Surface' pointing to the anvil, 3) Add 'First Printing: 2023' at the bottom center, and 4) Add 'Vol. IV' in the top right corner.



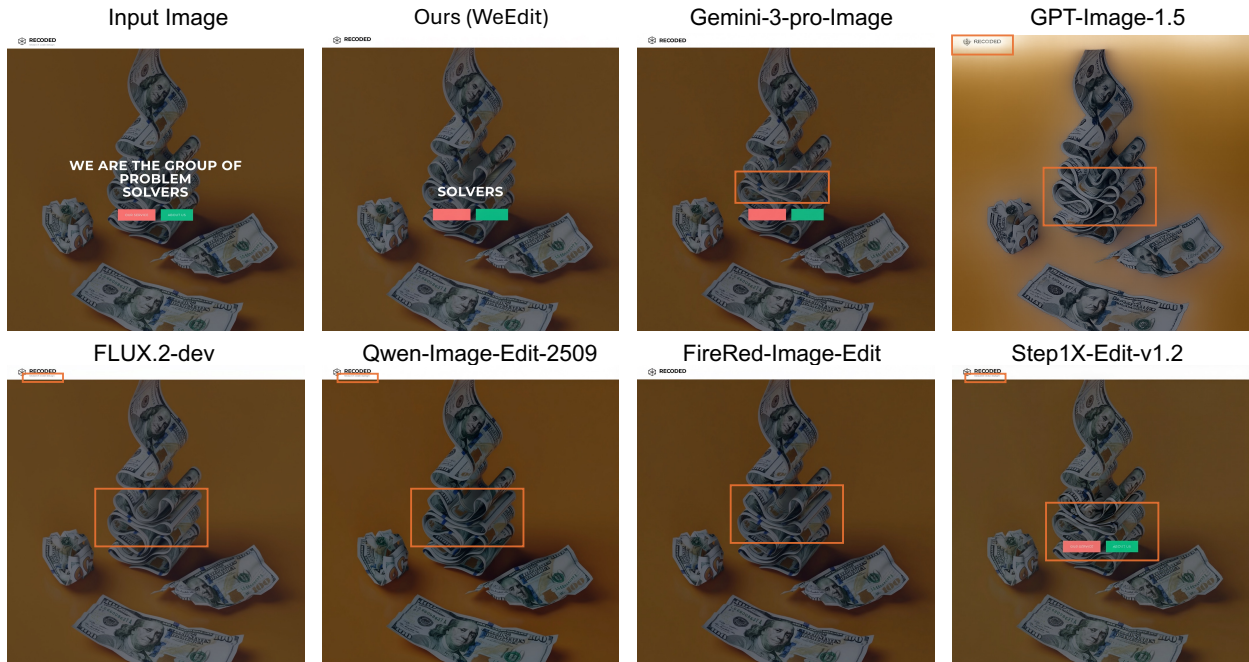
**Figure 8** Qualitative comparison of the **add** operation. Inaccurate instruction execution is highlighted with red boxes, unclear text rendering with purple boxes, and unintended alterations to non-editing regions with orange boxes.

1) Replace “STEEL FOSSIL: FROSTBITTEN” with “NEON DINO: CYBER WINTER”, 2) Replace “DAILY GACHA SUMMON” with “RARE HERO RECRUIT”, 3) Replace “SOLVE PUZZLE” with “START MISSION”, 4) Replace “CRYSTALS: 9,999” with “CREDITS: 5,000”, 5) Replace “MANA: 500/500” with “EXP: 850/1000”.



**Figure 9** Qualitative comparison of the **replace** operation. Inaccurate instruction execution is highlighted with red boxes, unclear text rendering with purple boxes, and unintended alterations to non-editing regions with orange boxes.

"Remove the texts: 'research code design', 'We Are The Group Of Problem', 'Our Service', 'About Us'"



"Rearrange 'Android Beam' with 'GPS Falso - Buscar localização', ensuring that their associated images also swap positions."

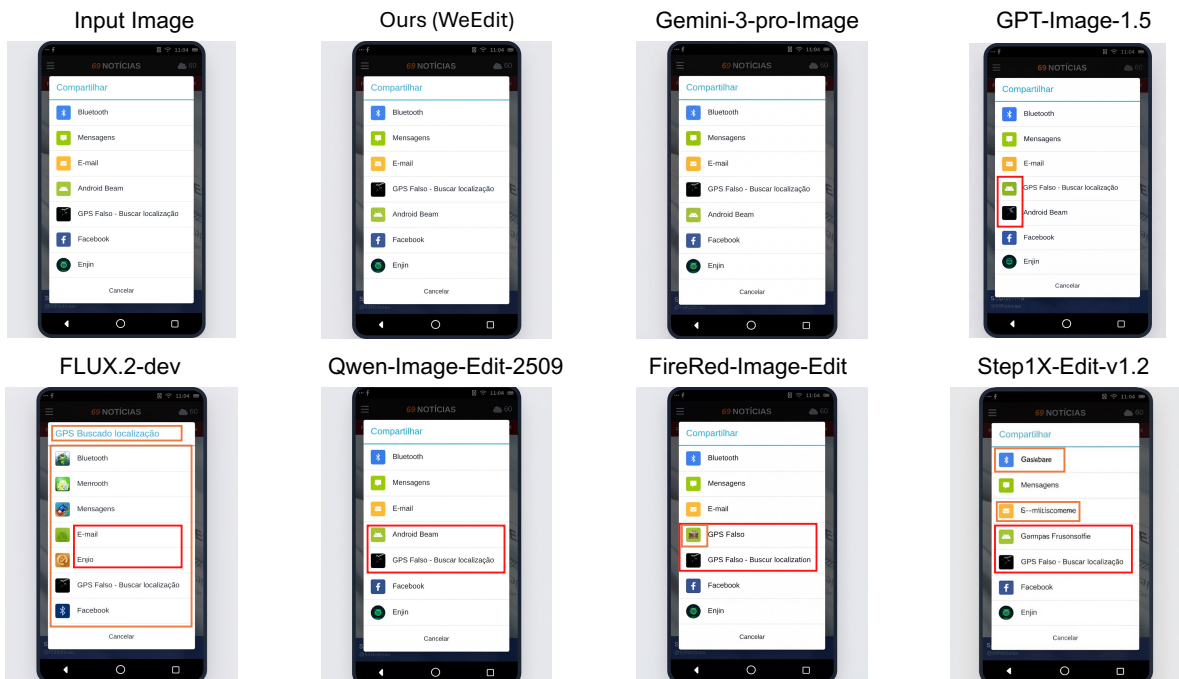


**Figure 10** Qualitative comparison of the **delete** and **rearrange** operations. Inaccurate instruction execution is highlighted with red boxes, unclear text rendering with purple boxes, and unintended alterations to non-editing regions with orange boxes.

"Translate all English text in this menu into Chinese. Every text element must be translated while maintaining the exact same layout, font size, and design. Numbers and prices should remain unchanged."

Input Image



Gemini-3-pro-Image



FLUX.2-dev



FireRed-Image-Edit



Ours (WeEdit)



GPT-Image-1.5



Qwen-Image-Edit-2509



Step1X-Edit-v1.2



**Figure 11** Qualitative comparison of the **translate** operation. Inaccurate instruction execution is highlighted with red boxes, unclear text rendering with purple boxes, and unintended alterations to non-editing regions with orange boxes.

"Change the color of the Arabic text ' عرق زروق ' to red."

Input Image



Gemini-3-pro-Image



FLUX.2-dev



FireRed-Image-Edit



Ours (WeEdit)



GPT-Image-1.5



Qwen-Image-Edit-2509



Step1X-Edit-v1.2



**Figure 12** Qualitative comparison of the **change style** operation. Inaccurate instruction execution is highlighted with red boxes, unclear text rendering with purple boxes, and unintended alterations to non-editing regions with orange boxes.

- 1) Replace the title “GLITCH MATE: CHRONOS” with “SYSTEM MALFUNCTION: CRITICAL FAILURE”,
- 2) Add the text “CONNECTION LOST” directly below the timer, 3) Swap the positions of the “EXECUTE STRATEGY” and “FORFEIT MATCH” buttons.

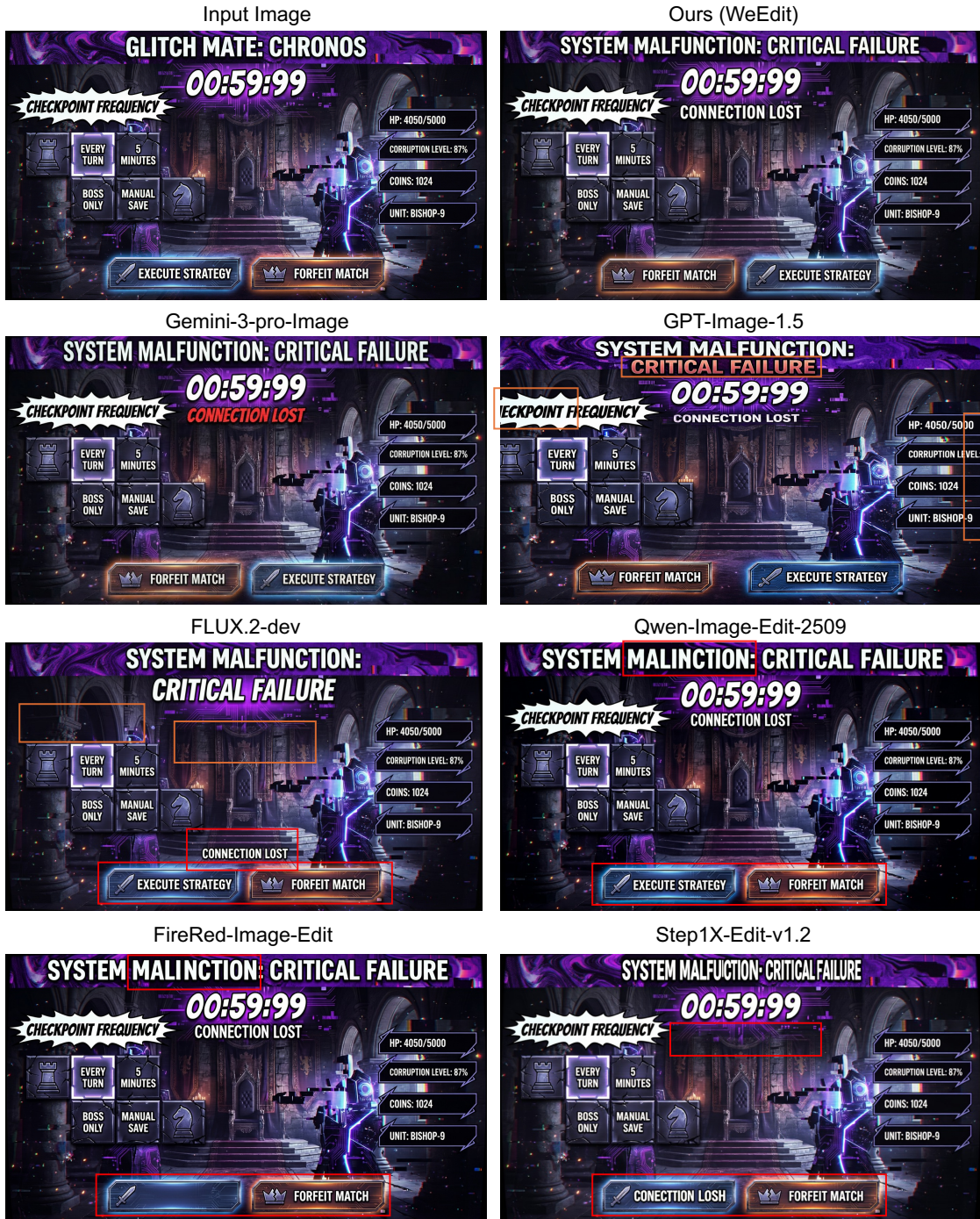
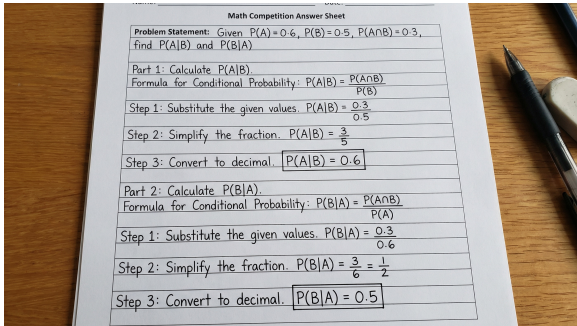


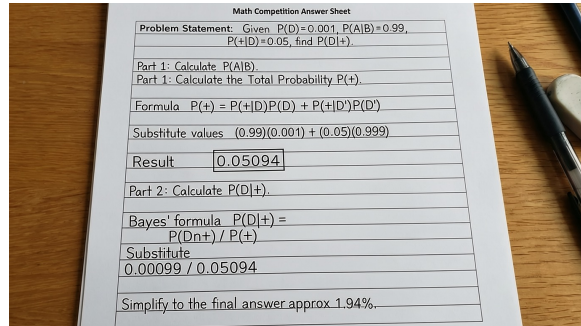
**Figure 13** Qualitative comparison of **combined** operations. Inaccurate instruction execution is highlighted with red boxes, unclear text rendering with purple boxes, and unintended alterations to non-editing regions with orange boxes.

"Replace the solution for 'P(A)=0.6, P(B)=0.5, P(A∩B)=0.3, find P(A|B) and P(B|A)' with the complete solution for 'Disease prevalence 0.1%, sensitivity 99%, false positive 5%, find P(disease|positive)'".

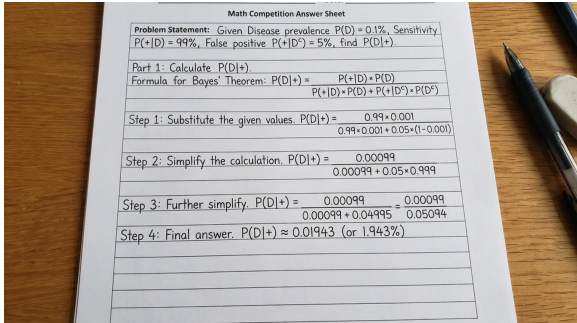
### Input Image



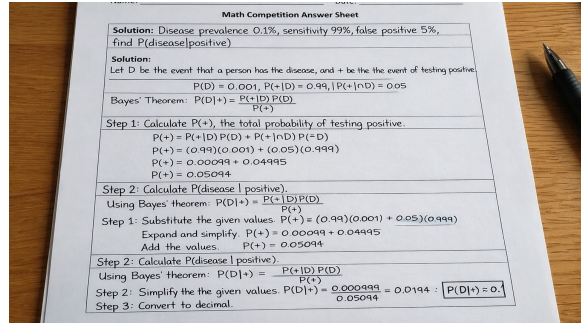
### Ours (WeEdit)



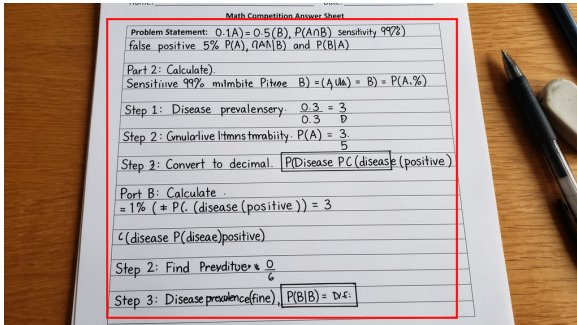
### Gemini-3-pro-Image



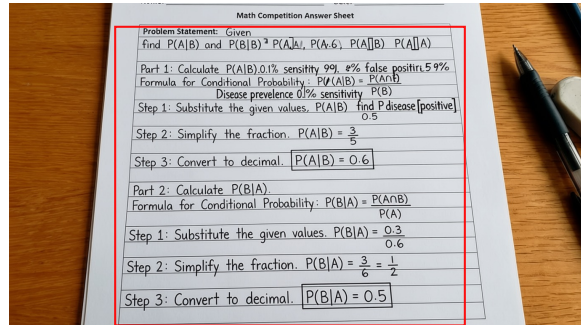
### GPT-Image-1.5



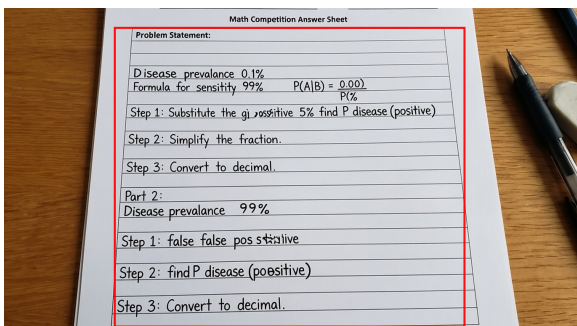
### FLUX.2-dev



### Qwen-Image-Edit-2509



### FireRed-Image-Edit



### Step1X-Edit-v1.2

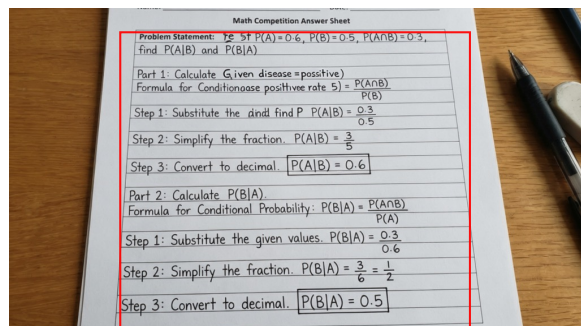


Figure 14 Qualitative comparison of the reasoning operation. Inaccurate instruction execution is highlighted with red boxes.

## References

- [1] Arial. <https://learn.microsoft.com/en-us/typography/fontlist/arial>.
- [2] Beautifulsoup4. <https://pypi.org/project/beautifulsoup4/>.
- [3] Pillow. <https://github.com/python-pillow/Pillow>.
- [4] Playwright. <https://github.com/microsoft/playwright>.
- [5] Tailwind. <https://tailwindcss.com/>.
- [6] Seedream4.5. [https://seed.bytedance.com/en/seedream4\\_5](https://seed.bytedance.com/en/seedream4_5), 2025.
- [7] Gemini-2.5-flash-image. <https://developers.googleblog.com/introducing-gemini-2-5-flash-image/>, 2025.
- [8] Gpt-image-1.5. <https://developers.openai.com/api/docs/models/gpt-image-1.5>, 2025.
- [9] Qwen-image-edit-2509. <https://huggingface.co/Qwen/Qwen-Image-Edit-2509>, 2025.
- [10] Qwen-image-edit-2511. <https://huggingface.co/Qwen/Qwen-Image-Edit-2511>, 2025.
- [11] Gemini-3.0-pro. <https://blog.google/products-and-platforms/products/gemini/gemini-3/>, 2025.11.
- [12] Gemini-3.0-pro-image. <https://blog.google/innovation-and-ai/technology/developers-tools/gemini-3-pro-image-developers/>, 2025.11.
- [13] Shuai Bai, Yuxuan Cai, Ruizhe Chen, Keqin Chen, Xionghui Chen, Zesen Cheng, Lianghao Deng, Wei Ding, Chang Gao, Chunjiang Ge, et al. Qwen3-vl technical report. [arXiv preprint arXiv:2511.21631](https://arxiv.org/abs/2511.21631), 2025.
- [14] Tim Brooks, Aleksander Holynski, and Alexei A Efros. Instructpix2pix: Learning to follow image editing instructions. In *CVPR*, 2023.
- [15] Qi Cai, Jingwen Chen, Yang Chen, Yehao Li, Fuchen Long, Yingwei Pan, Zhaofan Qiu, Yiheng Zhang, Fengbin Gao, Peihan Xu, et al. Hidream-1l: A high-efficient image generative foundation model with sparse diffusion transformer. [arXiv preprint arXiv:2505.22705](https://arxiv.org/abs/2505.22705), 2025.
- [16] Siyu Cao, Hangting Chen, Peng Chen, Yiji Cheng, Yutao Cui, Xinchu Deng, Ying Dong, Kipper Gong, Tianpeng Gu, Xiuse Gu, et al. Hunyuanimage 3.0 technical report. [arXiv preprint arXiv:2509.23951](https://arxiv.org/abs/2509.23951), 2025.
- [17] Di Chang, Mingdeng Cao, Yichun Shi, Bo Liu, Shengqu Cai, Shijie Zhou, Weilin Huang, Gordon Wetzstein, Mohammad Soleymani, and Peng Wang. Bytemorph: Benchmarking instruction-guided image editing with non-rigid motions. [arXiv preprint arXiv:2506.03107](https://arxiv.org/abs/2506.03107), 2025.
- [18] Jingye Chen, Yupan Huang, Tengchao Lv, Lei Cui, Qifeng Chen, and Furu Wei. Textdiffuser: Diffusion models as text painters. *NeurIPS*, 2023.
- [19] Jingye Chen, Yupan Huang, Tengchao Lv, Lei Cui, Qifeng Chen, and Furu Wei. Textdiffuser-2: Unleashing the power of language models for text rendering. In *ECCV*, 2024.
- [20] Junsong Chen, YU Jincheng, GE Chongjian, Lewei Yao, Enze Xie, Zhongdao Wang, James Kwok, Ping Luo, Huchuan Lu, and Zhenguo Li. Pixart- $\alpha$ : Fast training of diffusion transformer for photorealistic text-to-image synthesis. In *ICLR*, 2024.
- [21] Junying Chen, Zhenyang Cai, Pengcheng Chen, Shunian Chen, Ke Ji, Xidong Wang, Yunjin Yang, and Benyou Wang. Sharegpt-4o-image: Aligning multimodal models with gpt-4o-level image generation. [arXiv preprint arXiv:2506.18095](https://arxiv.org/abs/2506.18095), 2025.
- [22] Yufeng Cui, Honghao Chen, Haoge Deng, Xu Huang, Xinghang Li, Jirong Liu, Yang Liu, Zhuoyan Luo, Jinsheng Wang, Wenxuan Wang, et al. Emu3. 5: Native multimodal models are world learners. [arXiv preprint arXiv:2510.26583](https://arxiv.org/abs/2510.26583), 2025.
- [23] Chaorui Deng, Deyao Zhu, Kunchang Li, Chenhui Gou, Feng Li, Zeyu Wang, Shu Zhong, Weihao Yu, Xiaonan Nie, Ziang Song, et al. Emerging properties in unified multimodal pretraining. [arXiv preprint arXiv:2505.14683](https://arxiv.org/abs/2505.14683), 2025.
- [24] Prafulla Dhariwal and Alexander Nichol. Diffusion models beat gans on image synthesis. In *NeurIPS*, 2021.

- [25] Patrick Esser, Sumith Kulal, Andreas Blattmann, Rahim Entezari, Jonas Müller, Harry Saini, Yam Levi, Dominik Lorenz, Axel Sauer, Frederic Boesel, et al. Scaling rectified flow transformers for high-resolution image synthesis. In *ICML*, 2024.
- [26] Peng Gao, Le Zhuo, Ziyi Lin, Chris Liu, Junsong Chen, Ruoyi Du, Enze Xie, Xu Luo, Longtian Qiu, Yuhang Zhang, et al. Lumina-t2x: Transforming text into any modality, resolution, and duration via flow-based large diffusion transformers. *arXiv preprint arXiv:2405.05945*, 2024.
- [27] Yu Gao, Lixue Gong, Qiushan Guo, Xiaoxia Hou, Zhichao Lai, Fanshi Li, Liang Li, Xiaochen Lian, Chao Liao, Liyang Liu, et al. Seedream 3.0 technical report. *arXiv preprint arXiv:2504.11346*, 2025.
- [28] Feng Han, Yibin Wang, Chenglin Li, Zheming Liang, Dianyi Wang, Yang Jiao, Zhipeng Wei, Chao Gong, Cheng Jin, Jingjing Chen, et al. Unireditbench: A unified reasoning-based image editing benchmark. *arXiv preprint arXiv:2511.01295*, 2025.
- [29] Amir Hertz, Ron Mokady, Jay Tenenbaum, Kfir Aberman, Yael Pritch, and Daniel Cohen-Or. Prompt-to-prompt image editing with cross-attention control. In *ICLR*, 2023.
- [30] Jonathan Ho, Ajay Jain, and Pieter Abbeel. Denoising diffusion probabilistic models. In *NeurIPS*, 2020.
- [31] Edward J Hu, Yelong Shen, Phillip Wallis, Zeyuan Allen-Zhu, Yuanzhi Li, Shean Wang, Lu Wang, and Weizhu Chen. Lora: Low-rank adaptation of large language models. In *ICLR*, 2022.
- [32] Lianghua Huang, Wei Wang, Zhi-Fan Wu, Yupeng Shi, Huanzhang Dou, Chen Liang, Yutong Feng, Yu Liu, and Jingren Zhou. In-context lora for diffusion transformers. *arXiv preprint arXiv:2410.23775*, 2024.
- [33] Mude Hui, Siwei Yang, Bingchen Zhao, Yichun Shi, Heng Wang, Peng Wang, Cihang Xie, and Yuyin Zhou. Hq-edit: A high-quality dataset for instruction-based image editing. In *ICLR*, 2024.
- [34] Mengzhao Jia, Wenhao Yu, Kaixin Ma, Tianqing Fang, Zhihan Zhang, Siru Ouyang, Hongming Zhang, Dong Yu, and Meng Jiang. Leopard: A vision language model for text-rich multi-image tasks. *arXiv preprint arXiv:2410.01744*, 2024.
- [35] Diederik P Kingma. Auto-encoding variational bayes. *arXiv preprint arXiv:1312.6114*, 2013.
- [36] Yuval Kirstain, Adam Polyak, Uriel Singer, Shahbuland Matiana, Joe Penna, and Omer Levy. Pick-a-pic: An open dataset of user preferences for text-to-image generation. *NeurIPS*, 2023.
- [37] Black Forest Labs. Flux.1-dev. <https://blackforestlabs.ai/announcing-black-forest-labs>, 2024.
- [38] Black Forest Labs. Flux.2-dev. <https://huggingface.co/black-forest-labs/FLUX.2-dev>, 2025.
- [39] Black Forest Labs, Stephen Batifol, Andreas Blattmann, Frederic Boesel, Saksham Consul, Cyril Diagne, Tim Dockhorn, Jack English, Zion English, Patrick Esser, et al. Flux. 1 kontext: Flow matching for in-context image generation and editing in latent space. *arXiv preprint arXiv:2506.15742*, 2025.
- [40] Hugo Laurençon, Léo Tronchon, Matthieu Cord, and Victor Sanh. What matters when building vision-language models? *NeurIPS*, 2024.
- [41] Hugo Laurençon, Léo Tronchon, and Victor Sanh. Unlocking the conversion of web screenshots into html code with the websight dataset. *arXiv preprint arXiv:2403.09029*, 2024.
- [42] Junzhe Li, Yutao Cui, Tao Huang, Yinping Ma, Chun Fan, Miles Yang, and Zhao Zhong. Mixgrpo: Unlocking flow-based grpo efficiency with mixed ode-sde. *arXiv preprint arXiv:2507.21802*, 2025.
- [43] Zhimin Li, Jianwei Zhang, Qin Lin, Jiangfeng Xiong, Yanxin Long, Xincheng Deng, Yingfang Zhang, Xingchao Liu, Minbin Huang, Zedong Xiao, et al. Hunyuan-dit: A powerful multi-resolution diffusion transformer with fine-grained chinese understanding. *arXiv e-prints*, 2024.
- [44] Zongjian Li, Zheyuan Liu, Qihui Zhang, Bin Lin, Feize Wu, Shenghai Yuan, Zhiyuan Yan, Yang Ye, Wangbo Yu, Yuwei Niu, et al. Uniworld-v2: Reinforce image editing with diffusion negative-aware finetuning and mllm implicit feedback. *arXiv preprint arXiv:2510.16888*, 2025.
- [45] Bin Lin, Zongjian Li, Xinhua Cheng, Yuwei Niu, Yang Ye, Xianyi He, Shenghai Yuan, Wangbo Yu, Shaodong Wang, Yunyang Ge, et al. Uniworld-v1: High-resolution semantic encoders for unified visual understanding and generation. *arXiv preprint arXiv:2506.03147*, 2025.

- [46] Bingchen Liu, Ehsan Akhgari, Alexander Visheratin, Aleks Kamko, Linmiao Xu, Shivam Shrirao, Joao Souza, Suhail Doshi, and Daiqing Li. Playground v3: Improving text-to-image alignment with deep-fusion large language models. [arXiv preprint arXiv:2409.10695](#), 2024.
- [47] Jie Liu, Gongye Liu, Jiajun Liang, Yangguang Li, Jiaheng Liu, Xintao Wang, Pengfei Wan, Di ZHANG, and Wanli Ouyang. Flow-grpo: Training flow matching models via online rl. In [The Thirty-ninth Annual Conference on Neural Information Processing Systems](#), 2025.
- [48] Shiyu Liu, Yucheng Han, Peng Xing, Fukun Yin, Rui Wang, Wei Cheng, Jiaqi Liao, Yingming Wang, Honghao Fu, Chunrui Han, et al. Step1x-edit: A practical framework for general image editing. [arXiv preprint arXiv:2504.17761](#), 2025.
- [49] Xingchao Liu, Chengyue Gong, and Qiang Liu. Flow straight and fast: Learning to generate and transfer data with rectified flow. In [ICLR](#), 2023.
- [50] Zeyu Liu, Weicong Liang, Zhanhao Liang, Chong Luo, Ji Li, Gao Huang, and Yuhui Yuan. Glyph-byt5: A customized text encoder for accurate visual text rendering. In [ECCV](#), 2024.
- [51] Zeyu Liu, Weicong Liang, Yiming Zhao, Bohan Chen, Lin Liang, Lijuan Wang, Ji Li, and Yuhui Yuan. Glyph-byt5-v2: A strong aesthetic baseline for accurate multilingual visual text rendering. [arXiv preprint arXiv:2406.10208](#), 2024.
- [52] Cheng Lu, Yuhao Zhou, Fan Bao, Jianfei Chen, Chongxuan Li, and Jun Zhu. Dpm-solver: A fast ode solver for diffusion probabilistic model sampling in around 10 steps. [NeurIPS](#), 2022.
- [53] Jian Ma, Mingjun Zhao, Chen Chen, Ruichen Wang, Di Niu, Haonan Lu, and Xiaodong Lin. Glyphdraw: Seamlessly rendering text with intricate spatial structures in text-to-image generation. [arXiv preprint arXiv:2303.17870](#), 2023.
- [54] Jian Ma, Xujie Zhu, Zihao Pan, Qirong Peng, Xu Guo, Chen Chen, and Haonan Lu. X2edit: Revisiting arbitrary-instruction image editing through self-constructed data and task-aware representation learning. [arXiv preprint arXiv:2508.07607](#), 2025.
- [55] William Peebles and Saining Xie. Scalable diffusion models with transformers. In [CVPR](#), 2023.
- [56] Dustin Podell, Zion English, Kyle Lacey, Andreas Blattmann, Tim Dockhorn, Jonas Müller, Joe Penna, and Robin Rombach. Sdxl: Improving latent diffusion models for high-resolution image synthesis. In [ICLR](#), 2024.
- [57] Yusu Qian, Eli Bocek-Rivele, Liangchen Song, Jialing Tong, Yinfei Yang, Jiasen Lu, Wenze Hu, and Zhe Gan. Pico-banana-400k: A large-scale dataset for text-guided image editing. [arXiv preprint arXiv:2510.19808](#), 2025.
- [58] Robin Rombach, Andreas Blattmann, Dominik Lorenz, Patrick Esser, and Björn Ommer. High-resolution image synthesis with latent diffusion models. In [CVPR](#), 2022.
- [59] Nataniel Ruiz, Yuanzhen Li, Varun Jampani, Yael Pritch, Michael Rubinstein, and Kfir Aberman. Dreambooth: Fine tuning text-to-image diffusion models for subject-driven generation. In [CVPR](#), 2023.
- [60] Chitwan Saharia, William Chan, Saurabh Saxena, Lala Li, Jay Whang, Emily L Denton, Kamyar Ghasemipour, Raphael Gontijo Lopes, Burcu Karagol Ayan, Tim Salimans, et al. Photorealistic text-to-image diffusion models with deep language understanding. In [NeurIPS](#), 2022.
- [61] Jiaming Song, Chenlin Meng, and Stefano Ermon. Denoising diffusion implicit models. In [ICLR](#), 2021.
- [62] Richard S Sutton and Andrew G Barto. [Reinforcement learning: An introduction](#). MIT press, 2018.
- [63] Zhenxiong Tan, Songhua Liu, Xingyi Yang, Qiaochu Xue, and Xinchao Wang. Ominicontrol: Minimal and universal control for diffusion transformer. In [ICCV](#), pages 14940–14950, 2025.
- [64] Meituan LongCat Team, Hanghang Ma, Haoxian Tan, Jiale Huang, Junqiang Wu, Jun-Yan He, Lishuai Gao, Songlin Xiao, Xiaoming Wei, Xiaoqi Ma, et al. Longcat-image technical report. [arXiv preprint arXiv:2512.07584](#), 2025.
- [65] Super Intelligence Team, Changhao Qiao, Chao Hui, Chen Li, Cunzheng Wang, Dejie Song, Jiale Zhang, Jing Li, Qiang Xiang, Runqi Wang, et al. Firered-image-edit-1.0 technical report. [arXiv preprint arXiv:2602.13344](#), 2026.
- [66] Yuxiang Tuo, Wangmeng Xiang, Jun-Yan He, Yifeng Geng, and Xuansong Xie. Anytext: Multilingual visual text generation and editing. [arXiv preprint arXiv:2311.03054](#), 2023.

- [67] Juntong Wang, Jiarui Wang, Huiyu Duan, Jiayang Kang, Guangtao Zhai, and Xiongkuo Min. I2i-bench: A comprehensive benchmark suite for image-to-image editing models. [arXiv preprint arXiv:2512.04660](#), 2025.
- [68] Yuhan Wang, Siwei Yang, Bingchen Zhao, Letian Zhang, Qing Liu, Yuyin Zhou, and Cihang Xie. Gpt-image-edit-1.5 m: A million-scale, gpt-generated image dataset. [arXiv preprint arXiv:2507.21033](#), 2025.
- [69] Cong Wei, Zheyang Xiong, Weiming Ren, Xeron Du, Ge Zhang, and Wenhui Chen. Omniedit: Building image editing generalist models through specialist supervision. In [ICLR](#), 2024.
- [70] Jason Wei, Xuezhi Wang, Dale Schuurmans, Maarten Bosma, Fei Xia, Ed Chi, Quoc V Le, Denny Zhou, et al. Chain-of-thought prompting elicits reasoning in large language models. [NeurIPS](#), 2022.
- [71] Chenfei Wu, Jiahao Li, Jingren Zhou, Junyang Lin, Kaiyuan Gao, Kun Yan, Sheng-ming Yin, Shuai Bai, Xiao Xu, Yilei Chen, et al. Qwen-image technical report. [arXiv preprint arXiv:2508.02324](#), 2025.
- [72] Chenyuan Wu, Pengfei Zheng, Ruiran Yan, Shitao Xiao, Xin Luo, Yueze Wang, Wanli Li, Xiyan Jiang, Yexin Liu, Junjie Zhou, et al. Omnigen2: Exploration to advanced multimodal generation. [arXiv preprint arXiv:2506.18871](#), 2025.
- [73] Jay Zhangjie Wu, Xuanchi Ren, Tianchang Shen, Tianshi Cao, Kai He, Yifan Lu, Ruiyuan Gao, Enze Xie, Shiyi Lan, Jose M Alvarez, et al. Chronoedit: Towards temporal reasoning for image editing and world simulation. [arXiv preprint arXiv:2510.04290](#), 2025.
- [74] Keming Wu, Sicong Jiang, Max Ku, Ping Nie, Minghao Liu, and Wenhui Chen. Editreward: A human-aligned reward model for instruction-guided image editing. [arXiv preprint arXiv:2509.26346](#), 2025.
- [75] Shaojin Wu, Mengqi Huang, Wenxu Wu, Yufeng Cheng, Fei Ding, and Qian He. Less-to-more generalization: Unlocking more controllability by in-context generation. In [ICCV](#), 2025.
- [76] Shitao Xiao, Yueze Wang, Junjie Zhou, Huaying Yuan, Xingrun Xing, Ruiran Yan, Chaofan Li, Shuting Wang, Tiejun Huang, and Zheng Liu. Omnigen: Unified image generation. In [CVPR](#), 2025.
- [77] Jiazheng Xu, Xiao Liu, Yuchen Wu, Yuxuan Tong, Qinkai Li, Ming Ding, Jie Tang, and Yuxiao Dong. Imagereward: Learning and evaluating human preferences for text-to-image generation. [NeurIPS](#), 2023.
- [78] Zeyue Xue, Jie Wu, Yu Gao, Fangyuan Kong, Lingting Zhu, Mengzhao Chen, Zhiheng Liu, Wei Liu, Qiushan Guo, Weilin Huang, et al. Dancegrpo: Unleashing grpo on visual generation. [arXiv preprint arXiv:2505.07818](#), 2025.
- [79] Yukang Yang, Dongnan Gui, Yuhui Yuan, Weicong Liang, Haisong Ding, Han Hu, and Kai Chen. Glyphcontrol: Glyph conditional control for visual text generation. [NeurIPS](#), 2023.
- [80] Junyan Ye, Dongzhi Jiang, Zihao Wang, Leqi Zhu, Zhenghao Hu, Zilong Huang, Jun He, Zhiyuan Yan, Jinghua Yu, Hongsheng Li, et al. Echo-4o: Harnessing the power of gpt-4o synthetic images for improved image generation. [arXiv preprint arXiv:2508.09987](#), 2025.
- [81] Yang Ye, Xianyi He, Zongjian Li, Bin Lin, Shenghai Yuan, Zhiyuan Yan, Bohan Hou, and Li Yuan. Imgedit: A unified image editing dataset and benchmark. [arXiv preprint arXiv:2505.20275](#), 2025.
- [82] Qifan Yu, Wei Chow, Zhongqi Yue, Kaihang Pan, Yang Wu, Xiaoyang Wan, Juncheng Li, Siliang Tang, Hanwang Zhang, and Yueting Zhuang. Anyedit: Mastering unified high-quality image editing for any idea. In [CVPR](#), 2025.
- [83] Hui Zhang, Dexiang Hong, Yitong Wang, Jie Shao, Xinglong Wu, Zuxuan Wu, and Yu-Gang Jiang. Creatilayout: Siamese multimodal diffusion transformer for creative layout-to-image generation. In [ICCV](#), 2025.
- [84] Hui Zhang, Dexiang Hong, Maoke Yang, Yutao Cheng, Zhao Zhang, Jie Shao, Xinglong Wu, Zuxuan Wu, and Yu-Gang Jiang. Creatidesign: A unified multi-conditional diffusion transformer for creative graphic design. In [ICLR](#), 2026.
- [85] Kai Zhang, Lingbo Mo, Wenhui Chen, Huan Sun, and Yu Su. Magicbrush: A manually annotated dataset for instruction-guided image editing. [NeurIPS](#), 2023.
- [86] Zechuan Zhang, Ji Xie, Yu Lu, Zongxin Yang, and Yi Yang. Enabling instructional image editing with in-context generation in large scale diffusion transformer. In [NeurIPS](#), 2025.
- [87] Zhao Zhang, Yutao Cheng, Dexiang Hong, Maoke Yang, Gonglei Shi, Lei Ma, Hui Zhang, Jie Shao, and Xinglong Wu. Creatiposter: Towards editable and controllable multi-layer graphic design generation. [arXiv preprint arXiv:2506.10890](#), 2025.

- [88] Haozhe Zhao, Xiaojian Shawn Ma, Liang Chen, Shuzheng Si, Rujie Wu, Kaikai An, Peiyu Yu, Minjia Zhang, Qing Li, and Baobao Chang. Ultraedit: Instruction-based fine-grained image editing at scale. NeurIPS, 2024.
- [89] Xiangyu Zhao, Peiyuan Zhang, Kexian Tang, Xiaorong Zhu, Hao Li, Wenhao Chai, Zicheng Zhang, Renqiu Xia, Guangtao Zhai, Junchi Yan, et al. Envisioning beyond the pixels: Benchmarking reasoning-informed visual editing. arXiv preprint arXiv:2504.02826, 2025.
- [90] Yiming Zhao and Zhouhui Lian. Udifftext: A unified framework for high-quality text synthesis in arbitrary images via character-aware diffusion models. In ECCV, 2024.
- [91] Kaiwen Zheng, Huayu Chen, Haotian Ye, Haoxiang Wang, Qinsheng Zhang, Kai Jiang, Hang Su, Stefano Ermon, Jun Zhu, and Ming-Yu Liu. Diffusionnft: Online diffusion reinforcement with forward process. arXiv preprint arXiv:2509.16117, 2025.
- [92] Wendi Zheng, Jiayan Teng, Zhuoyi Yang, Weihang Wang, Jidong Chen, Xiaotao Gu, Yuxiao Dong, Ming Ding, and Jie Tang. Cogview3: Finer and faster text-to-image generation via relay diffusion. In ECCV, 2024.
- [93] Dewei Zhou, You Li, Fan Ma, Zongxin Yang, and Yi Yang. Migc++: Advanced multi-instance generation controller for image synthesis. TPAMI, 2024.
- [94] Dewei Zhou, You Li, Fan Ma, Xiaoting Zhang, and Yi Yang. Migc: Multi-instance generation controller for text-to-image synthesis. In CVPR, 2024.
- [95] Dewei Zhou, Mingwei Li, Zongxin Yang, and Yi Yang. Dreamrenderer: Taming multi-instance attribute control in large-scale text-to-image models. In ICCV, pages 16712–16722, 2025.